

## Point-to-point response to reviewers' comments

*The comments are in black, and our answers are in blue.*

### Reviewer #2:

#### Summary:

This manuscript examines the impact of sea ice changes on the surface air and sea temperatures in the Arctic during the Pliocene, as simulated by EC-Earth. Specifically, they examine the energy flux impact of differences in surface albedo and surface ocean insulation spatially correlated with the changes in sea ice between the Pliocene and pre-industrial eras. They found that a reduction in albedo allows for much stronger short-wave heating during May, causing the biggest SST difference between the two eras to be during August. They also found that this extra stored heat was released back to the atmosphere via enhanced surface heat fluxes due to the decrease in sea ice insulation. This resulted in SAT differences between the two eras being largest during winter, and with an inverse seasonal timing relative to SST.

#### Paper recommendation:

Understanding how sea ice influences Arctic climate, particularly for higher-CO<sub>2</sub> forcing scenarios, is of great importance in terms of understanding what our future climate state will be. The Pliocene also provides a unique test bed to examine sea ice in a warm climate, given that it was in near-equilibrium with a similar forcing compared to now, along with enough proxy data to validate model results. Thus I do believe this paper is a beneficial contribution to the literature. However, I do have some concerns in regards to the interpretation of their results, particularly sea ice's influence on clouds and water vapor. I also believe there needs to be some grammatical improvements to the text itself, to help make the manuscript easier to read. Given this, I am recommending **Major Revisions**. Although I hope these revisions are not too difficult to implement, I do believe they will significantly improve the final manuscript.

*We are grateful for the positive evaluation and constructive comments that follow.*

#### Major issues:

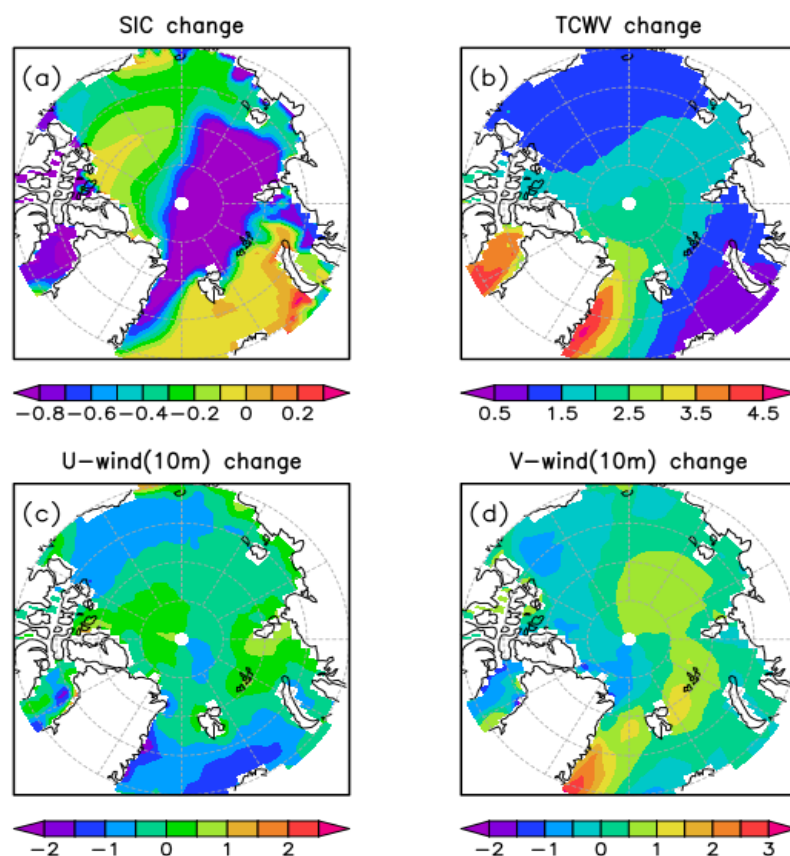
1. I am worried that some of the changes, especially related to water vapor and cloud cover, may not be directly related to changes in sea ice, but instead are related to a third variable that is also correlated with the sea ice (which would produce the correlation you found). The reason for this concern is that (I believe) you are using multi-year temporal averages to calculate the spatial correlation. However, over those

time-scales potentially significant changes in the large-scale circulation could be present, which would impact clouds, water vapor, and sea ice through, for example, changes in atmospheric and oceanic heat transport. I sadly don't know of a great way to untangle all of these effects, but I could imagine calculating the correlation between sea ice and, say, vertically-integrated atmospheric moisture and heat flux, to see if it changed substantially in regions with substantial sea ice loss, or regions with noticeable changes in water vapor/cloud cover.

If that correlation analysis produces a relationship that is difficult to interpret, then I would at least add a plot showing the annual average differences between atmospheric heat and moisture fluxes, or at least wind fields, to help the reader understand how the atmospheric circulation over the Arctic is different in the Pliocene relative to the pre-industrial.

Related to this, are your correlations and analyses including the entire Arctic, or just the regions that have or had sea ice? If you are examining the entire Arctic, then I might recommend examining only the sea ice regions, as there appears to be large surface heat flux changes in regions that contain little-to-no sea ice in both eras, which could be contaminating the statistical relationships between sea ice and the associated surface flux changes.

The differences of sea ice concentration, total column water vapour and wind fields at 10m over the Arctic in the Pliocene relative to the preindustrial are shown below.



There is no significant correlation between sea ice concentration and wind fields at 10m ( $r_{\text{sic,uwnd}}=-0.06$ ,  $r_{\text{sic,vwnd}}=-0.22$ ). The total column water vapour is the combination of local source and large-scale circulation transport, and the former is correlated with sea ice concentration, which might lead to a weak correlation ( $r=-0.44$ ) between SIC and total column water vapour. As you mentioned, a variety of processes are tangled, so in the study we attempted to decompose into individual contribution by CFRAM and EFA-like method.

Our correlations and analyses are including the entire Arctic except for turbulent heat fluxes. Note that ice-free and ice-covered are classified by the threshold of 15% sea ice concentration as commonly used in sea ice study. The ice-covered regions in both eras are examined in the revised manuscript as suggested.

2. I would strongly recommend having a native or very-proficient English speaker edit this document, as there are a large number of minor but noticeable grammatical errors, such as missing articles (a, an, the), and misuses of pluralization, combined with some strange phrasing that made the document difficult to understand sometimes. By improving the grammar/wording, I believe this manuscript would be made much stronger and more accessible to a wider audience.

We have corrected the grammatical errors. A native English speaker has proofread the revised manuscript.

#### **Minor issues:**

1. Are all the maps shown in this manuscript annual averages? If so this should be stated in the text (you mention it in a few locations in the text, just not everywhere). Yes, all the maps shown are annual averages. We have stated “annual mean” in the text and figure captions.

2. It is interesting in your supplemental figure that the net TOA is negative (implying energy loss), yet all the surface variables show increasing warming. Does this imply a cooling higher up in the atmosphere, and thus a change in the atmospheric lapse rate (which could impact clouds and water vapor)?

We agree. The negative TOA flux and the positive net surface energy fluxes in the EC-Earth simulation (also shown in ERA-Interim, Hazeleger et al., 2011) might possibly affect the atmospheric lapse rate. It is interesting but beyond the scope of this paper and could be investigated in the further study.

3. The modeled SSTs do well in the Atlantic, but quite poor in the (North) Pacific. Could this imply a bias in the Pacific basin, which could impact heat fluxes coming

from the Pacific into the Arctic? Just a short sentence or two on it would be all that I would recommend.

The overlay of proxy data over the filled contour maps does not clearly show the difference, therefore we show the difference of annual mean SST anomaly (Pliocene minus preindustrial) between EC-Earth simulation and the proxy data in Figure S2. The underestimation in high latitude regions, similar to multi-model mean in Dowsett et al. (2012) but significantly less in bias, is found both in the Atlantic and in the North Pacific. Thus it is difficult to confirm the impact on heat fluxes coming from the Pacific into the Arctic.

4. It would help to include the striping and cross-hatching in Figure 2f as well, so the reader can see how the surface heat flux changes with respect to the sea ice transitions.

Done.

5. How does sea ice thickness change in the regions where sea ice is still present in the Pliocene?

We found that sea ice thickness would show a decline and reduce the surface albedo due to the warming in Pliocene. The decrease in the surface albedo due to a decrease in the fractional sea ice coverage (sea ice concentration) is focused on in this paper, and the decrease in the sea-ice albedo due to melting ice (sea ice thickness change) is mentioned in section 4. It can be found from section 4 that the former is dominant when they affect the net shortwave radiation at the surface.

6. I assume the correlation shown in Figure 5 is significant, but it would still be good to state that somewhere in the text (as a high r-squared value doesn't always imply significance).

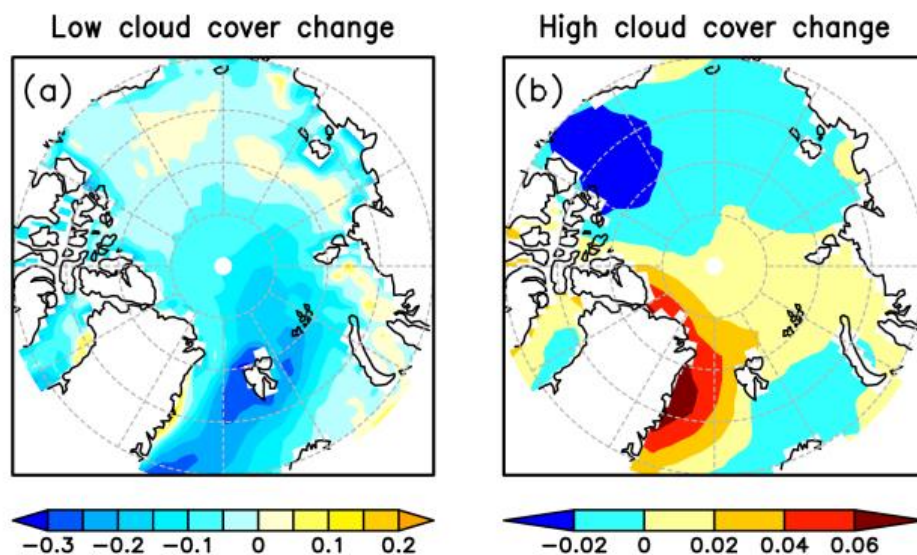
The statistical significance of the correlation coefficient is stated in the revised version.

7. Line 252: If sea ice insulation reduces local water vapor and cloud cover, then it could certainly impact the local surface radiation budget, at least in the long-wave. Not sure if this sentence was just not worded correctly?

The sentences are confusing and they have been rewritten in the revised version as “By separating the overlying atmosphere from the ocean, sea ice reduces evaporation from the ocean, resulting in a decrease in water vapour and cloud cover. This reduction plays a non-negligible role in the amount of downward shortwave and longwave radiation reaching the surface. However, remote moisture transport also affects water vapour and cloud amount.”.

8. It would help to show how the actual cloud cover is changing over the Arctic in the Pliocene (just showing cloud fraction by low and high clouds would help). That would put the changes shown in Figure 7 into better context.

The low and high cloud cover changes are shown below (See also Figure S3). The significant decrease of low cloud cover in North Atlantic may enhance incoming shortwave radiation and weaken downwelling longwave radiation, thus contributing to the positive anomaly in shortwave radiation (Figure 7a) and negative anomaly in longwave radiation (Figure 7b) in North Atlantic. Similarly, the increase of high cloud cover east and north of Greenland is responsible for the positive anomaly in longwave radiation (Figure 7b) over the related areas. These analyses are added in the revised text and Figure S3.



9. It would be beneficial to see a spatial map of the latent and sensible heat flux changes, similar to Figures 2 and 3.

A spatial map of the latent and sensible heat flux changes has been shown in Figure 3c and 3d.

10. Figure 8: Any idea as to why the longwave cloud forcing in September is so large relative to all the other months? Again, just a sentence or two would probably be all that is needed.

The mean cloud cover over the Arctic peaks in September, which contributes to large longwave radiation changes. In addition, there is a significant linear relationship between sea ice concentration and longwave radiation changes due to cloud in

September. Therefore the the longwave cloud forcing in September is much larger than in the other months. We have added this explanation in the last paragraph of Section 5.1.

# Contribution of sea -ice albedo and insulation effects to Arctic amplification in the EC-Earth Pliocene simulation

Jianqiu Zheng<sup>1,2,3</sup>, Qiong Zhang<sup>1</sup>, Qiang Li<sup>1</sup>, Qiang Zhang<sup>1</sup>, Ming Cai<sup>4</sup>

<sup>1</sup>Department of Physical Geography and Bolin Centre for Climate Research, Stockholm University, Stockholm, 10691, Sweden

<sup>2</sup>School of Earth and Space Sciences, University of Science and Technology of China, Hefei, 230026, China

<sup>3</sup>Key Laboratory of Meteorological Disaster of Ministry of Education, Nanjing University of Information Science and Technology, Nanjing, 210044, China

<sup>4</sup>Department of Earth, Ocean and Atmospheric Science, Florida State University, Tallahassee, Florida, 32306, USA

Correspondence to: Jianqiu Zheng (qiu@ustc.edu.cn)

**Abstract.** In the present work, we simulate the Pliocene climate with ~~the~~ EC-Earth climate model as an ~~analogue~~equilibrium state for current warming climate induced by rising CO<sub>2</sub> in the atmosphere. The simulated Pliocene climate shows a strong Arctic amplification ~~featured-by~~featuring pronounced warming sea surface temperature (SST) over ~~the~~ North Atlantic, in particular over Greenland Sea and Baffin Bays, which is comparable with geological SST reconstructions from ~~the Pliocene Research, Interpretation and Synoptic Mapping group (PRISM-, Dowsett et al., 2016)~~. To understand the underlying physical processes, the air-sea heat flux variation in response to Arctic sea -ice change is quantitatively assessed by a climate feedback and response analysis method (CFRAM) and an ~~approach similar to~~ equilibrium feedback assessment-~~(EFA)-like approach-~~Giving. Given the ~~facts~~fact that the maximum SST warming ~~in-SST~~ occurs in summer while the maximum ~~warming-in~~ surface air temperature warming happens during winter, our analyses show that a dominant ice-albedo effect is the main reason for summer SST warming, and a 1% loss in sea -ice concentration could lead to an approximate 21.8 Wm<sup>-2</sup> increase in shortwave solar radiation into open sea surface. During winter ~~month~~months, the insulation effect induces enhanced turbulent heat flux out of ~~the~~ sea surface due to sea -ice melting in previous summer months. This leads to more heat ~~releaser~~released from the ocean to atmosphere, thus explaining ~~the-stronger~~why surface air temperature warming amplification is stronger in winter than in summer.

## 1 Introduction

~~Through~~As shown in the monitoring at Mauna Loa Observatory in Hawaii (<https://www.esrl.noaa.gov/gmd/obop/mlo/>), the CO<sub>2</sub> concentration in the atmosphere ~~had steadily~~ passed ~~the~~ 400 ppm threshold by September 2016. Accordingly, global mean temperature in 2016 increased by about 1.1 °C compared to ~~that-of~~the preindustrial period, as released by the World Meteorological Organization (<https://public.wmo.int/en/media/press-release>), ~~one~~. One major consequence of this continuing and accelerating warming is the rapid melting of ice ~~in~~at high latitudes. ~~Ten~~The ten lowest minimum Arctic sea -ice extents since satellite records were made available in 1979 have ~~taken place in recent~~happened in every year of the last



decade except for 2005, as documented by National Snow and Ice Data Centre. Moreover, ~~an~~ ice-free Arctic Ocean is estimated to emerge ~~in~~ around 2050 on the basis of climate model projections (Overland et al., 2011). As ~~the~~ sea -ice retreats, ~~its reflectivity~~ the surface of the Arctic Ocean becomes less reflective and ~~insulation decrease~~ the enhanced open-ocean region leads to greater air-sea heat exchange due to the reduced insulating effect of sea ice. This leads to ~~the~~ changes in the surface heat budget, and ~~the~~ changes in overlying cloud and water vapour, further ~~amplify the~~ amplifying Arctic warming and sea -ice melting. Many studies have shown that the accelerated Arctic sea -ice retreat ~~is~~ possibly ~~resulted~~ results from local ice-albedo positive feedback (Winton, 2008), meridional heat transport by atmospheric circulation and oceanic current (Alexeev et al., 2013), or sea -ice drift out of the Fram Strait (Nghiem et al., 2007; Krumpen et al., 2016). In turn, Arctic sea -ice decline can result in a variety of impacts on climate change, such as Arctic amplification (Serreze et al., 2009), change of cloud cover and precipitation (Liu et al., 2012; Bintanja and Selten, 2014), shift in atmospheric circulation pattern (Alexander et al., 2004), and slow-down of the Atlantic Meridional Overturning Circulation (Sévellec et al., 2017). A detailed consequence of Arctic sea -ice decline classified by local and remote effects ~~have~~ has been reviewed by Vihma et al. (2014).

Such ongoing high CO<sub>2</sub> level and low ice concentration in ~~the~~ Arctic is not unique in Earth's history. Geological data show that during the Pliocene, the CO<sub>2</sub> concentration in the atmosphere ~~did reach~~ reached 400 ppm or even more, and extreme warmth and Arctic amplification are recorded in multi-proxy evidence, including the longest and most complete record from Lake El'gygytyn, an undisturbed Siberian lake in northeast Arctic Russia (Brigham-Grette et al., 2013). Seasonally ice-free conditions existed in some Arctic regions in the mid-Pliocene until ~~the~~ circulation through the Bering Strait reversed ~~and, at which point~~ the excess freshwater supply might have facilitated sea -ice formation (Matthiessen et al., 2009). Several climate models have simulated the Pliocene but failed to reproduce the strong Arctic amplification ~~showed~~ shown in geological proxy data (Dowsett et al., 2012). While most of ~~the~~ previous studies on ~~contribution~~ the contributions of the sea -ice effect to Arctic amplification focus on contemporary ~~trend~~ trends or future ~~projection~~ projections, here the Pliocene simulation is selected ~~because of~~ for three reasons: (1) The Pliocene epoch (~~~~~ (approximately 3 million years ago), the most recent warm period with ~~the CO<sub>2</sub> concentrations~~ similar CO<sub>2</sub> concentration ~~as~~ to today, is not only an analogue of future climate change but also an appropriate past time-slice to examine ~~regarding~~ sea -ice effect (Haywood et al., 2016a). (2) The Pliocene simulation can be partly verified by proxy data reconstructed from deep-sea oxygen isotope analysis (Dowsett et al., 2012), while ~~projecting~~ the future ~~projection~~ from a climate model is of high uncertainty owing to the lack of any validation. (3) Whereas the historical or undergoing climate variability is transient, the Pliocene simulation is obtained after the model integration reaches a quasi-equilibrium ~~state~~. As inferred from Li et al. (2013), the equilibrium response is in principle reversible, while transient response is hysteretic, suggesting that the Pliocene simulation can better represent a steady climate response.

Two physical ~~attributions~~ characteristics of sea -ice are considered to affect climate system. One is much higher surface reflectivity of ice than that of open water, and the other is that ice can inhibit or reduce the exchange of momentum, heat, and mass between the atmosphere and ocean, ~~hereafter~~. Hereafter we refer these two ~~attribution~~ effects as "albedo" and



“insulation-effects,” respectively. Most previous studies on the two effects are mainly carried out by sensitivity experiments with the atmospheric general circulation model (AGCM). For instance, Gildor et al. (2014) examined the role of sea-ice ~~on~~in the hydrological cycle using the Community Atmospheric General Circulation Model (CAM3). ~~Two~~The two effects are separated by modifying the sea-ice albedo to that of open-water, or setting the sea-ice thickness to zero ~~but its albedo and~~ keeping albedo unchanged. Their results show that the insulation effect on the hydrological cycle is larger than the albedo effect, and these two effects are not independent, i.e. their total effect is not the sum of their separate contribution. Lang et al. (2017) also pointed out that the sea-ice thinning in recent years can lead to a 37% increase ~~37%~~ of Arctic amplification through the enhanced insulation effect, as estimated by an AGCM. Note that sea surface temperature (SST) is prescribed in their AGCM simulation, while sea-ice albedo or thickness is modified. In fact, the modification of sea-ice does not closely match the fixed SST ~~closely~~, which may lead to a bias in the sea-ice effect estimation from the AGCM simulation. The climate system, in turn, reinforces sea-ice loss while influenced by albedo or insulation ~~effect~~effects, which ~~is~~are known as ice-albedo feedback or ice-insulation feedback. In addition, albedo ~~effect~~ and insulation ~~effect~~ ~~interacts~~interact in a nonlinear way (Gildor et al., 2014). These feedbacks and ~~interaction~~interactions add more challenges to ~~understand~~understanding the effect of sea-ice on climate. Recently, Burt et al. (2016) and Kim et al. (2016) addressed the relationship between sea-ice loss and air-sea interface heat budget using the Community Earth System Model (CESM) simulation and cyclo-stationary empirical orthogonal function (CSEOF) analysis, respectively. However, the studies contain large uncertainties due to the hysteresis of transient processes (Li et al., 2013). Although the surface heat budget is the most fundamental ~~to aspect of~~ air-sea interaction, it is still not clear to what ~~degree~~extent heat flux responds to the change of Arctic sea-ice. Therefore the present study aims to quantitatively assess the variation of each individual component of air-sea heat flux caused by the decrease of Arctic sea-ice albedo and insulation. The analysis is based on the EC-Earth simulation of the Pliocene climate, which ~~representing~~represents an analogue for a future climate at equilibrium ~~climate with~~ modern greenhouse gas levels, and the reference state is preindustrial equilibrium climate state.

The remainder of the paper is organized as follows. Section 2 describes the EC-Earth model and experimental design, and introduces the climate feedback and response analysis method (CFRAM) ~~),~~ as well as the approach to extract the impact ~~contributed from~~ of sea-ice loss. In ~~section~~Section 3, we present several climate features simulated in the Pliocene experiment. The albedo and insulation effects of sea-ice on air-sea interface heat flux are investigated in Sections 4 and 5, respectively ~~in sections 4 and 5,~~ followed by summary and discussion in ~~section~~Section 6.

## 2 Model and method

### 2.1 Model description and experimental design

The model applied in the study is the global coupled climate model EC-Earth (version 3.1, Hazeleger et al., 2012). Its atmospheric component is the Integrated Forecast System (IFS, version cycle 36r4) developed at the European Centre for Medium-Range Weather Forecast (ECMWF), including the land model H-TESSEL (Balsamo et al., 2009). This atmospheric

spectral model is run at T159 resolution (roughly 1.125°, ~~~approximately~~ 125 km) with 62 vertical levels and coupled to ~~thean~~ ocean component ~~that is~~ based on the Nucleus for European Modelling of the Ocean (NEMO, version 3.3, Madec, 2008) and the Louvain-la-Neuve sea-ice Model (LIM, version 3, Vancoppenolle et al. 2009). ~~The~~ NEMO ~~iswas~~ developed at the Institute Pierre Simon Laplace (IPSL) and has a resolution of about 1° and 46 vertical levels. In LIM3, surface albedo parameterization follows Shine and Henderson-Sellers (1985) with the following values: thick dry snow 0.8, thick melting snow 0.65, thick frozen bare ice 0.72, thick melting bare ice 0.53, and thin melting ice 0.47. The tuning of bare ice and snow albedo would affect whether the equilibrium ice thickness is reasonable and whether the ice is from a multi-year or seasonal ice zone. The coupling between the atmosphere and ocean/sea-ice is through the Ocean Atmosphere Sea-ice Soil coupler (OASIS, version 3.0, Valcke, 2006). EC-Earth has been used to examine the Arctic climate for the historical period and future scenarios in CMIP5. An evaluation of EC-Earth for the Arctic shows that the model simulates the 20th century Arctic climate reasonably well. EC-Earth simulated cloud variables with slightly larger cloud fraction and less cloud condensate ~~compared-tothan~~ ERA-Interim, which ~~leadled~~ to similar longwave cloud radiative forcing. Moreover, total cloud forcing in EC-Earth is in good agreement ~~toewith~~ the APP-x satellite estimates (Koenigk et al., 2013). Koenigk et al. (2013) showed that the annual mean surface temperature in the Arctic increases by 12 K in the EC-Earth RCP8.5 scenario simulation, and the most pronounced warming is during autumn and winter in the lower atmosphere. A likely ice-free Arctic is indicated in September around 2040. The enhanced oceanic meridional heat flux into the Arctic (Koenigk et al., 2013) and the enhanced atmospheric northward latent energy transport (Graversen and Burtu, 2016) are suggested as major contributors to ~~the~~ future Arctic warming in the EC-Earth simulation. ~~Recently-the~~ The EC-Earth model ~~ishas~~ also been applied to understand ~~the~~ past ~~elimateclimates~~, such as changes in the-change-of Arctic climate (Muschitiello et al., 2015), African ~~monsoonmonsoons~~ (Pausata et al., 2016; Gaetani et al., 2017), tropical ~~eyelonecyclones~~ (Pausata et al., 2017a)), and ENSO activity (Pausata et al., 2017b) during the mid-Holocene. In this study we apply the model to the mid-Pliocene climate and focus on the effects of sea-ice on Arctic climate change.

Two numerical experiments are performed with EC-Earth to facilitate this study. One is the preindustrial control run with the 1850 CO<sub>2</sub> concentration of 284.725 ppm, and the other is the mid-Pliocene warm period (3.264–3.025 Ma) sensitivity experiment in which the atmospheric CO<sub>2</sub> concentration is set to 400 ppm. Following the protocol of the Pliocene Model Intercomparison Project, phase 2 (PlioMIP2, Haywood et al., 2016b), several configurations are modified in the Pliocene simulation: (1) in the Pliocene experiment, all ~~other~~ trace gases ~~exceptother than~~ CO<sub>2</sub>, such as CH<sub>4</sub> ~~and~~ N<sub>2</sub>O, and aerosols ~~in the Pliocene experiment~~, are specified ~~to-beas~~ identical to the preindustrial run to account for the absence of proxy data. (2) Orbit forcing, including eccentricity, obliquity, and precession, remains same within the preindustrial run as in the mid-Pliocene warm period, which has a near-modern orbital forcing. (3) Enhanced boundary ~~conditionconditions~~ from the Pliocene Research, Interpretation and Synoptic Mapping group (PRISM, Dowsett et al., 2016)), including land-sea mask, topography, bathymetry, and ice-sheet, are applied in the Pliocene experiment ~~where the land-sea mask, orography, bathymetry, vegetation~~. The global distributions of lake, soil, and ice-sheetbiome are modified accordingly to match the new land-sea mask and ice reconstruction. The integrations of the preindustrial control run and the Pliocene experiment are

carried out for 500 years, and it takes ~~approximate~~approximately 300 years for ~~the~~ model to reach equilibrium. From our last 200 years ~~of~~ output in the Pliocene simulation (see Figure S1 in the Supplement), the mean top of the atmosphere (TOA) net radiation is about  $-0.5 \text{ Wm}^{-2}$  and its trend is near zero. The trend of mean SST is about 0.027 K/century, which fulfils the PMIP4 criterion that the trend of mean SST should be less than 0.05 K/century (Kageyama et al., 2018). In this study, the last 100-year-mean of all variables are used for analysis, and the Pliocene climate anomalies are calculated ~~with respect to by subtracting the mean of the preindustrial control run. The Arctic insimulation without trends removal.~~ In the following analysis, the Arctic is defined as the region poleward of 70 °N.

## 2.2 Climate feedback and response analysis method (CFRAM)

~~Radiative forcing varies as CO<sub>2</sub> concentration increases~~Climate system warming in the Pliocene experiment is driven by variation in radiative forcing, which ~~drives climate system warming is in turn caused by increased CO<sub>2</sub> concentration.~~ In response to temperature change, factors such as surface albedo, cloud, water vapour, and air temperature will adjust and feedback until the climate system reaches equilibrium. The contribution from each factor can be quantitatively evaluated by climate feedback analysis. ~~The traditional~~Traditional climate feedback analysis ~~method~~methods, such as partial radiative perturbation ~~(PRP) technique~~, is based on TOA radiative budget (Wetherald and Manabe, 1988), while the radiative kernel method can be extended to the surface and remain computationally efficient (Soden and Held, 2006; Pithan and Mauritsen, 2014). However, none of them takes individual physical processes into account, particularly non-radiative processes. ~~The climate feedback and response analysis method (CFRAM),~~ proposed by Lu and Cai (2009), overcomes this limitation.

CFRAM contains two parts: one is decomposing radiative perturbation into individual contribution, including shortwave and longwave components, from CO<sub>2</sub>, surface albedo, cloud, water vapour, and air temperature. ~~It:~~

$$\Delta Q_{rad} = \Delta(S + R)_{CO_2} + \Delta S_{albedo} + \Delta(S + R)_{cloud} + \Delta(S + R)_{WV} + \Delta R_T, \quad (1)$$

where  $\Delta Q_{rad}$  is performed by offline calculation using total radiative transfer model (Fu and Liou, 1993) with flux perturbation at the output from surface (ice and ocean),  $\Delta S$  and  $\Delta R$  are the preindustrial control run and net shortwave and longwave radiative perturbations at the Pliocene sensitivity experiment surface, respectively, and the subscripts CO<sub>2</sub>, albedo, cloud, WV, and T represent the partial radiative perturbation due to changes in the CO<sub>2</sub> concentration, surface albedo, cloud properties, atmospheric water vapour, and air temperature, respectively. Note that here it is assumed that the interactions among the factors (CO<sub>2</sub>, surface albedo, cloud, water vapour, and air temperature) are negligible and the higher order terms of each factors are omitted. The other part is calculating partial ~~temperatetemperature~~ perturbation due to individual radiative and non-radiative feedback processes, which is based on total energy balance and derived from the relationship between longwave radiation and temperature change. A more detailed description about CFRAM can be found in Lu and Cai (2009).

CFRAM is a practical diagnostic tool to ~~analyze~~analyse the role of various forcing and feedback agents and has been used widely in climate change research (e.g. Taylor et al., 2013; Song and Zhang, 2014; Hu et al., 2017). In the present study,

total radiative flux perturbation is first calculated from the surface radiative flux difference between the Pliocene sensitivity experiment and the preindustrial control run. Then we apply the first part of CFRAM to ~~obtain the surface radiative flux~~ compute each partial radiative perturbation, which is performed by offline calculation using a radiative transfer model (Fu and Liou, 1993). The linear approximation in Equation (1) should be verified with the output from the radiative transfer model. Finally, the partial radiative perturbation due to albedo, cloud, and water vapour, ~~and link it can be used~~ to evaluate albedo or insulation ~~effeteffects~~ of sea -ice.

### 2.3 Approach to extract sea -ice effects

As sea -ice declines in the Pliocene warming climate, ~~air-sea~~ heat flux ~~at air-sea interface~~ varies. However, the variation is not only due to the impact of sea -ice but also determined by other factors, such as atmospheric circulation. Therefore an approach capable of quantifying the influence of a factor is indispensable ~~to extract~~for extracting the corresponding ~~part~~contribution of sea -ice effect from the total heat flux change. To distinguish sea -ice's contribution from the other processes, the linkage between sea -ice and heat flux needs to be identified through either temporal correlation or spatial correlation, if the effect of sea -ice is assumed to be linear. A canonical case of the former is ~~the~~ equilibrium feedback assessment (EFA) ~~method,~~, which has been used to quantify the influence of sea -ice on cloud cover (Liu et al., 2012) and the heat flux response to SST (Frankignoul and Kestenare, 2002).

Here we adopt a method similar to EFA, but built on spatial correlation due to the limitation of data and computation. As a high-temporal-resolution CFRAM calculation, such as 6-hourly or daily, is computationally expensive, monthly data are used in the analysis. However, the monthly resolution is too coarse to explain the relationship between heat fluxes and sea-ice concentration by temporal correlations. Therefore, spatial correlations are calculated. This method is used in Hu et al. (2017) to correct cloud feedback. The response of heat flux to ~~change~~changes in sea -ice concentration (SIC) is represented as

$$F(s) = \lambda I(s) + N(s), \quad (4)2)$$

where  $F(s)$  is the heat flux anomaly at location  $s$ ,  $I(s)$  is anomalous SIC,  $\lambda$  is the response coefficient of heat flux to SIC change, and  $N(s)$  is the climate noise independent of SIC variability. The response coefficient can be calculated as

$$\lambda = \frac{cov[F(s), I(s)]}{cov[I(s), I(s)]}, \quad (2)3)$$

where  $cov[F(s), I(s)]$  is the spatial covariance between heat flux and SIC, and  $cov[I(s), I(s)]$  is the spatial variance of SIC.

The statistical significance of response coefficient is tested using a two-sided Student's t-test, where the effective degree of freedom is estimated from the auto-correlation function (Bretherton et al., 1999) as

$$n = N \frac{1-r_1 r_2}{1+r_1 r_2}, \quad (34)$$

where  $n$  is the effective degree of freedom,  $N$  is the sample size, and  $r_1$  is the lag-one auto-correlation of heat flux ~~and~~ (similarly  $r_2$  for SIC). Note that auto-correlation of heat flux and SIC is so strong that  $r_1$  and  $r_2$  can approach 1, leading to a ~~drastieally~~drastic decrease of effective degree of freedom.

Unlike the ~~present earth~~modern Earth observation system, the Pliocene climate proxy data are reconstructed mainly from the ~~benthic~~benthic-oxygen isotope analysis of deep-sea samples, such as foraminifera, diatom, and ostracod assemblages. Several climate features have been revealed with the multi-proxy data, ~~one~~ (Haywood et al., 2016a). ~~One of the most concern is permanent El Niño-like condition during the mid Pliocene warm period (Wara et al., 2005; Federov et al, 2006), which points out that the SST difference between the western and eastern equatorial Pacific was absent or less evident, similar to the contemporary El Niño SST pattern while not happening on interannual timescale. The other characteristic concerning~~ is Arctic amplification — the warming in surface air temperature (SAT) in the Arctic region tends to be more than twice as warm as that in the low- and mid-latitude ~~region~~regions (Serreze and Barry, 2011). ~~However, the~~Furthermore, Arctic SAT and SST during Pliocene is significantly warmer than today ~~even though they have, despite~~ comparable CO<sub>2</sub> ~~concentration~~concentrations (Ballantyne et al., 2013), ~~which~~. This probably stems from the ~~fact that the~~ present transient process ~~that~~ has not yet reached a steady state, or is due to the change of ~~the~~ gateways that can affect the Atlantic meridional overturning circulation (AMOC) (Brierley and Fedorov, 2016; Otto-Bliesner et al., 2017; Feng et al., 2017).

In Figure 1, we show the ~~changes in annual mean warming and seasonal warming averaged over the Arctic Ocean for~~ SST and SAT between the ~~Pliocene and preindustrial period and the Pliocene epoch simulations~~. The shaded circles in the SST change distribution (Figure 1a) represent the mean annual SST anomalies at 95% confidence-assessed marine sites from ~~the~~ Deep Sea Drilling Project (~~DSDP~~) and Ocean Drilling Program (~~ODP~~), which are available in the supplementary table of Dowsett et al. (2012). ~~The overlay of proxy data over the filled contour maps does not show the difference well, so the difference of annual mean SST anomaly between EC-Earth simulation and the proxy data is shown in Figure S2.~~ In contrast to the large underestimation of multi-model ensembles ~~to~~regarding the warming over the northern Atlantic sector of the Arctic Ocean (Dowsett et al., 2012), the warming amplitude and pattern in EC-Earth simulation is comparable with the high-confidence proxy data. This is consistent with the ~~results~~result of Koenigk et al. (2013), which ~~pointed out~~suggests that the sea ice change in EC-Earth is strong and ~~that the~~ EC-Earth simulations show a strong Arctic amplification compared to most CMIP3 models. ~~Meanwhile, a warming can be seen along the coastal upwelling zones off the America, which implies a permanent El Niño-like feature.~~ According to Figure 1b, the Pliocene SAT north of 70 °N is as much as 10–18 °C higher than the preindustrial period, similar to ~~the~~ mid-Pliocene paleoclimate estimate by Robinson et al. (2008).

~~Figure~~Figures 1a and 1b also show that the SST and SAT anomaly patterns are somewhat similar over low- and mid-latitude ~~region, but they are apparently~~regions, different from over high-latitude ~~region~~regions, particularly over the Arctic Ocean, which ~~is~~was previously illustrated by Hill et al. (2014). This disparity results from the intense air–sea coupling over tropical and subtropical ~~ocean~~oceans, while the air–sea interaction is relatively weak over the Arctic Ocean owing to the albedo and insulation effects of sea ice. ~~Noteworthy, the~~Notably, SST warming ~~of SST~~ averaged over the Arctic Ocean shows a distinct seasonal evolution from that of SAT, ~~and~~; the maximum warming in SST occurs in summer, while the maximum warming in SAT happens during winter (FigureFigures 1c and 1d).

The SIC is very sensitive during the different period as shown in Figure 2a-e. During the preindustrial period, the annual mean sea ice appears to cover the whole Arctic Ocean except for the Greenland Sea, the Norwegian Sea, and the Barents Sea, and it retreats to the western Arctic Ocean in the Pliocene, leading to a significant decrease of sea ice extent over the Fram Basin and Baffin Bay (Figures 2a-c). Consequently, the net air-sea interface heat exchange at the surface of ice or ocean varies greatly (Figure 2d-f). The sea ice-f. The net heat flux and other flux terms mentioned hereafter are defined as positive downward. A positive value means that the ocean gains heat from the atmosphere and a negative value means oceanic heat loss. The net heat flux over the sea ice-covered area seems to be clearly shows net heat loss during both the preindustrial period and the Pliocene (Figures 2d and 2e). Thus, it can be expected that net heat gain will occur when the sea ice declines. However, the Fram Basin and Baffin Bay displays display pronounced heat loss, which might be linked to the disappearance of sea ice in the Pliocene (Figure 2b).

The net heat flux at the air-sea interfaces surface of ice or ocean can be written represented as

$$Q_{net} = Q_{sw} + Q_{lw} + Q_{sh} + Q_{lh}, \quad (4)$$

Where  $Q_{sw}$  and  $Q_{lw}$  are the sum of four terms: the net solar shortwave and radiative flux, the net longwave radiative heat fluxes,  $Q_{sh}$  and  $Q_{lh}$  are flux, the turbulent sensible heat flux, and the turbulent latent heat fluxes. All terms are defined positive downward. Therefore, the positive value means that ocean gains heat from the atmosphere and the negative value means oceanic heat loss.

Figure 3 compares the annual mean of the four components of surface heat flux terms to further illustrate the possible relationship between sea ice and net heat exchange (Figure Figures 2c and 2f). The radiative and turbulent heat fluxes flux anomalies both are positive over the Chukchi Sea, thereby indicating a marked net heat gain emerging there. Over the Beaufort Sea and East Siberian Sea, the positive change in the net shortwave radiation is anomalies are dominant over the other three negative components, yielding the net heat gain. On the contrary In contrast, the positive net shortwave radiation anomalies over the Fram Basin, the Greenland Sea, and Baffin Bay is are less than the sum of net longwave radiation and turbulent heat fluxes flux anomalies, thus leading to net heat loss. The negative turbulent heat fluxes flux anomalies over Fram Basin, the Greenland Sea, and Baffin Bay are so prominent, indicating the sea ice effect on turbulent heat fluxes flux anomalies in light of the transition to ice-covered or ice-free state states, respectively. As shown in Note that the partition threshold of ice-free and ice-covered conditions is 15% SIC, i.e., a grid point with an SIC of less than 15% is considered ice-free. In Figure 2c, the diagonal stripe represents the region with the transition from ice-covered to ice-free condition, and the diagonal crosshatch represents the region remaining that retains its ice-covered status as the simulation shifts from the preindustrial period to the Pliocene. Only ice-covered regions are examined, as there appears to be large surface heat flux changes in regions that contain no sea ice in both periods, which could be contaminating the statistical relationships between sea ice and the associated surface flux changes.

#### 4 Albedo effect of sea -ice

Arctic amplification has been demonstrated by significant SAT anomalies in the foregoing Pliocene simulation, ~~and it can be accounted as the synergy of CO<sub>2</sub>-external forcing and feedback effects associated with.~~ Similar to the process-based decomposition of a climate difference in Hu et al. (2017), the SAT anomalies in the Pliocene simulation as compared to the preindustrial simulation can be thought of as the combination of partial temperature perturbations due to radiative feedbacks (surface albedo, cloud, water vapour, and air temperature,) and non-radiative feedbacks (surface sensible and latent heat fluxes, dynamical advection, ocean processes, etc.). That is to say, the albedo effect of sea -ice and snow can be quantified by climate feedback analysis such as CFRAM. ~~The surface~~ Surface albedo is defined as the ratio ~~proportion~~ of the ~~reflected to the incoming incident~~ solar shortwave radiation that is reflected by the surface, therefore indicating that albedo effect is relevant ~~with to net~~ shortwave radiation rather than net longwave radiation and turbulent heat fluxes.

The annual mean net shortwave radiation change due to sea -ice and snow albedo derived from CFRAM is presented in Figure 4. The largest net shortwave radiation change exceeding  $50 \text{ Wm}^{-2}$  takes place over ~~the~~ Fram Basin and Baffin Bay, and most of the Arctic Ocean, except for part of ~~the~~ North Atlantic and the Barents Sea ~~show, shows net~~ shortwave radiative heat gain. ~~Comparing~~ Compared with the SIC change (Figure 2c), the increase of annual mean net shortwave radiation absorbed by the ocean is in accordance with sea -ice retreat, which can be clearly depicted in a scatter plot (Figure 5). ~~The high~~ The effective degree of freedom is calculated from Formula (4) for testing statistical significance, and the correlation coefficient ( $r = -0.9284$ ) is significant at a 99% confidence level. This indicates that changes in sea -ice extent can explain the approximate 84.71% (square of correlation coefficient) variance of total shortwave radiation change due to albedo, and the residual variance may be caused by changes in snow cover ~~or and~~ sea -ice/snow state as well as thickness. The statistically significant response coefficient calculated according to formula (23) is ~~-46.5-43.0~~  $\text{Wm}^{-2}$  ~~(exceeding 99% confidence level),~~ indicating that a 1% decrease in annual mean SIC leads to an approximate 0.543  $\text{Wm}^{-2}$  increase in net shortwave radiative heat flux at the surface.

~~Regarding the seasonal variation of~~ As SIC and ~~the~~ incoming solar radiation ~~are distinct~~ in the polar region vary with season, we examine the response of net shortwave radiation to sea -ice change for every month. As shown in Figure 6, the response coefficient of albedo to SIC displays a seasonal variation, peaking in ~~which it peaks in May~~ June with ~~the~~ maximum absolute value ~~188.4 of 178.3~~  $\text{Wm}^{-2}$  (approximate 21.8  $\text{Wm}^{-2}$  increase in net shortwave radiation due to 1% decrease in SIC). The prominent oceanic heating in May and June seems ~~inconsistent~~ consistent with the maximum SST warming in August, as the response of seawater lags about 2 months behind due to the great heat inertia and heat capacity of seawater (Venegas et al., 1997; Zheng et al., 2014). Even though Arctic sea -ice itself has a great variability owing to melting and freezing processes, ~~the~~ SIC anomalies do not exhibit a large variability in different seasons, ranging from 0.3419 to 0.4426 as shown in the standard deviation of SIC (Table 1). However, the standard deviation of net shortwave radiation anomalies (with respect to monthly mean) associated with albedo effect varies from 88.4352.45  $\text{Wm}^{-2}$  in May to  $0 \text{ Wm}^{-2}$  in December, when the polar night ~~occurring~~ occurs without any sunlight. Moreover, ~~it is found from our~~ correlation analysis



indicates that sea -ice has a statistically significant impact on surface shortwave radiation, except in November, December, and January, when there is low incident solar shortwave radiation during the Arctic winter. Overall, the seasonality of sea ice's albedo effect of sea-ice on surface shortwave radiation is attributed primarily to the seasonal cycle of net shortwave radiation, and the contribution of sea-ice SIC variation is substantially small.

## 5 Insulation effect of sea -ice

### 5.1 Insulation effect of sea -ice on surface radiation

The insulating effect of sea -ice, has an indirect effect on the net surface shortwave and longwave fluxes. By separating the overlying atmosphere from the ocean, does not affect surface shortwave or longwave radiation directly. In fact, the sea ice reduces the evaporation from the ocean to atmosphere, resulting in a decrease of in water vapour and cloud cover, and thus playing. This reduction plays a non-negligible role on in the amount of downward shortwave and longwave radiation reaching the surface radiation. However, the water vapour and cloud contain a mixture of local evaporation and remote moisture transport. In also affects water vapour and cloud amount. Thus, in order to address the insulation effect of sea -ice, two steps have to be performed. First, we obtain the total influence of water and cloud on surface radiation by CFRAM. Second, we need to extract the contribution from a local source associated with sea -ice.

Figure 7 shows the annual mean cloud feedback and water vapour feedback on net shortwave and longwave radiation, respectively, before removing the remote effects on clouds and water vapour. Even though the increase in cloud cover is expected with the diminishing Arctic sea -ice (Liu et al., 2012), whether the increased cloud cover will heat or cool the surface depends on the cloud characteristics of cloud. The cloud feedback on shortwave radiation is nearly out of phase with that on longwave radiation, except in the Beaufort Sea and the East Siberian Sea (Figure 7a, 7b). The significant decrease of low cloud cover in the North Atlantic (Figure S3a) may enhance incoming shortwave radiation and weaken downwelling longwave radiation, thus contributing to the positive anomaly in shortwave radiation and negative anomaly in longwave radiation in the North Atlantic. Similarly, the increase of high cloud cover east and north of Greenland (Figure S3b) is responsible for the positive anomaly in longwave radiation over the related areas. In contrast, the water vapour feedback tends to simultaneously cool and heat the surface by absorbing solar radiation and heat the surface by downwelling longwave radiation, and respectively; the latter heating is one order of magnitude higher than the former cooling (Figure 7c, 7d).

The approach to extract the counterpart of sea-ice local insulation effect due to changes in sea ice concentration is based on the premise that the insulation effect on surface radiation is linear with SIC. Like the steps performed into isolate the albedo effect, the response coefficient of shortwave and longwave radiation due to cloud and water vapour for annual mean and seasonal evolution can be calculated respectively, and the results are shown in Figure 8. As to In the annual mean, the main contributor comes from cloud feedback on longwave radiation ( $-12.6(-11.1 \text{ Wm}^{-2})$ ), and the cloud feedback on shortwave radiation and water vapour feedback on longwave radiation are similar in magnitude, but opposite in sign. In addition, the annual mean absorption of incoming solar radiation by water vapour is negligible, and this is true for the

individual month as well. The absorption and reflection of shortwave radiation by cloud ~~represents~~ shows a pronounced seasonal cycle, with a large effect in July and August. However, there is no statistically significant relationship between SIC and cloud feedback on shortwave radiation and SIC (Table 2). Comparing Compared to the seasonal variation of shortwave radiation change, standard deviation of the net shortwave radiation anomalies, standard deviation of the net longwave radiation anomalies caused by cloud and water vapour associated with local SIC anomalies both show smaller seasonal variation, therefore leading to a relatively constant contribution of sea-ice insulation to surface longwave radiation, except in summer months when there is a lack of significant interaction linear relationship between SIC and longwave radiation (Table 2). Note that the longwave cloud forcing in September ( $-17.6 \text{ Wm}^{-2}$ ) is quite large relative to all the other months, which might result from the maximum cloud cover over the Arctic, as well as the fact that the linear relationship between sea ice concentration and longwave radiation changes due to cloud is strongest in September.

## 5.2 Insulation effect of sea-ice on turbulent heat fluxes

The air-sea turbulent heat fluxes, including sensible and latent heat fluxes, have been widely studied with the bulk aerodynamic formula, which specifies that the turbulent heat fluxes are dependent on surface wind speed, sea surface and air temperature difference, specific humidity difference, and the bulk heat transfer coefficient. However, due to the existence of sea-ice, the Arctic turbulent heat fluxes show distinctive features from ice-free conditions, which has been mentioned in Section 3. It is therefore essential to take the insulation effect of sea-ice into account and differentiate ice-covered fluxes from ice-covered versus ice-free areas. This is demonstrated in Figure 9, which displays the Pliocene anomalies in annual mean sensible and latent heat flux change fluxes as a function of SIC anomalies. There are is a larger spread of spread in the turbulent heat flux change anomalies over the ice-free areas (grey symbols, corresponding to the diagonal hatched region in Figure 2c) than that of in anomalies from the ice-covered areas (light blue symbols, cross-hatched region in Figure 2c) because the former is free from the constraint of sea-ice. The constraint of sea-ice can be apparently captured through the scatter plot of turbulent heat flux and changes in SIC change (the light blue plot in Figure 9, corresponding to the diagonal crosshatch symbols). For the ice-covered areas in Figure 2c, and, SIC can explain approximate 59% and 74% (square of correlation coefficient) of the variance in the sensible heat flux and latent heat flux, respectively.

The linear regressions of sensible and latent heat flux anomalies on SIC are similar but different. The response coefficient of sensible heat flux ( $35.3 \text{ Wm}^{-2}$ ) to SIC is larger than that of latent heat flux ( $27.7 \text{ Wm}^{-2}$ ), for the ice-covered areas, which means that the sensible heat flux is more sensitive to SIC change than the latent heat flux. Noteworthy Notably, this is different from the turbulent heat flux variability over low- and mid-latitude regions, where the trend variability of sensible heat flux is significantly less than that of latent heat flux (e.g., such as the trend of turbulent heat flux over the low- and mid-latitude North Pacific and North Atlantic oceans from 1984–2004 (Li et al., 2011)). The positive intercept on the turbulent flux anomaly axis implies more heat gain at the sea surface, even if there is now without SIC change. Because the large specific heat capacity of seawater leads to less warming of the ocean than of the atmosphere, therefore the sea surface and air temperature difference or (the specific humidity difference) decreases induring the cold season when the turbulent

heat transport is the most pronounced, and consequently resulting in the lessa lower annual heat loss from the ocean to the atmosphere.

Figure 10 shows the seasonal response coefficient of the sensible and latent heat fluxes to the sea-ice. Apparently two SIC. It appears that the turbulent heat fluxes have thea similar seasonal evolution, peaking in November and showing a negative response in July. Therefore the maximum warming of SAT occurs in November as a consequence of, the prompt atmospheric prompt response to turbulent heating is an important contributing factor to the maximum SAT warming that occurs in November. The melting of sea-ice due to warming by high levels of CO<sub>2</sub> can attenuate the insulation effect and result in more heat transfer through the processes of conduction or evaporation from the ocean to the atmosphere when SST is higher than SAT; therefore, the turbulent heat fluxes correlate positively with SIC in all seasons except summer (Table 3). If SAT is higher than SST, (for instance, in July the), sea -ice will inhibit the heat transfer from the atmosphere to ocean; thus, the negative correlation emerges. However, the correlations between the turbulent heat fluxes and SIC in summer are not statistically significant (Table 3), indicating other factors might be dominant rather than sea -ice might be dominant.

## 6 Summary and discussion

In the present work we attempt to understand the albedo and insulation effects of sea-ice, on a warm Arctic climate during Pliocene simulated by EC-Earth coupled model. In contrast to Arctic amplification in the Pliocene has previously been addressed from reconstructed data (e.g. Robinson et al., 2008; Brigham-Grette et al., 2013); however these data tell only part of the story because of a scarcity of data sites. A model may be applied to investigate mechanisms and processes that help understanding. In contrast to the underestimation of multi-model ensembles documented in Dowsett et al. (2012), the EC-Earth Pliocene simulation can better display some main features manifested in the characteristics that have been revealed by the paleoclimate proxy data from deep-sea oxygen isotope analysis. Thus the EC-Earth coupled model is used in the present work to simulate the Pliocene climate and study the contribution of sea ice albedo and insulation to Arctic amplification in Pliocene had been confirmed by reconstructed data (e.g. Robinson et al., 2008; Brigham-Grette et al., 2013). Proxy data, however, tell only part of the story. Thus a model is applied and it can reveal the complete picture with reasonable explanation.

As a key to reveal the important features of Arctic amplification, the air-Air-sea heat flux variation in response to Arctic sea -ice change is quantitatively assessed by CFRAM and an EFA-like method: in order to reveal important features of Arctic amplification. Table 4 summarizes the results presented in sectionSections 4 and 5, which separately illustratedillustrate the effects of changes in albedo and insulation of sea -ice on surface heat exchange. Annual mean and seasonal evolution of effects are both considered, and. These allow us to partly interpret the mechanisms of Arctic amplification because the results are merely the contribution from sea -ice change. A complete energy budget, including dynamical and thermodynamical processes, is required to understand Arctic amplification comprehensively. The Pliocene Arctic amplification compared to the preindustrial simulation represents a maximum SST warming in August and expected to partly interpret the variability of heat flux.

390 —~~The albedo~~ maximum SAT warming in November, which might be associated with the albedo and insulation effects of  
~~sea ice. Albedo~~ only regulates the shortwave radiation, and its effect is primarily determined by annual cycle of insolation.  
 As sea -ice melts ~~from starting in~~ early spring, the enhanced insolation through open sea surface makes the ocean warmer,  
 with the most pronounced heating ~~anomalies~~ in May and June. Because of the great heat inertia and heat capacity of  
 seawater, ~~the SST warming anomaly~~ peaks in August. As a result of ~~the~~ albedo effect of sea -ice, ocean heat content increases  
 395 and more heat is stored in the upper ocean, which is the potential for the later enhanced heat release from ocean to  
 atmosphere. The insulation effect of sea -ice can ~~indirectly~~ modulate ~~not only~~ shortwave and longwave radiation ~~anomalies~~  
 indirectly through cloud and water vapour, ~~but also as well as directly modulate~~ sensible and latent heat ~~fluxes directly flux~~  
~~anomalies~~, since sea -ice serves as a barrier. Averaged over the year, the absorption of longwave radiation due to insulation  
 effect is about 4 times stronger than the reflected shortwave radiation by cloud, while the contribution of water vapour to  
 400 shortwave radiation is almost negligible. The longwave radiation ~~change anomalies~~ in response to cloud and water vapour is  
 attributed to downwelling longwave radiation, as upwelling longwave radiation depends solely on the surface temperature  
 according to the Stefan–Boltzmann law, and its seasonal variation is relatively small compared to the significant seasonality  
~~showing~~ in shortwave radiation. The ~~Pliocene~~ sea -ice decline ~~accelerates, as compared to the preindustrial period, amplifies~~  
 the turbulent exchange between the ocean and atmosphere, and the annual sum of sensible and latent heat ~~fluxes exceed flux~~  
 405 ~~anomalies exceeds~~ radiation ~~fluxes flux anomalies~~. In particular, heat is released to the atmosphere by the prominent  
 enhanced turbulent heat ~~fluxes flux anomalies~~ in ~~winter, amplifying the atmospheric warming~~ November, contributing to the  
~~formation of the maximum SAT anomaly in November.~~

~~A synthesis of Arctic amplification given by Serreze and Barry (2011) has introduced some of the physical processes~~  
~~mentioned above, including sea ice loss, albedo feedback, cloud cover, and water vapour. Unlike Serreze and Barry (2011),~~  
 410 ~~in this work we apply CFRAM and an EFA-like method to untangle these physical processes and obtain a quantitative~~  
~~understanding of sea-ice effects, which would help to directly evaluate the impact on heat exchange once the sea-ice~~  
~~concentration variation within Arctic is given. The EC-Earth simulation shows a stronger Arctic amplification than multi-~~  
~~model ensembles (Dowsett et al., 2012). However, an underestimation of Arctic warming as compared to proxy data remains~~  
~~in the EC-Earth simulation, implying less warmth produced by the EC-Earth model from oceanic heat transport, which~~  
 415 ~~yields a clue for improving the simulation. Furthermore, caution should be exercised when discussing sea-ice effects on heat~~  
~~flux, as underestimating Arctic warming might affect the interface heat exchange.~~

Though significant albedo and insulation effects of sea -ice have been studied, the possible nonlinear response of heat flux  
 to sea -ice can not be captured in this work. In addition, ~~the this~~ approach to ~~extract extracting~~ sea -ice effects is based on ~~the~~  
 spatial correlation; whether the corresponding conclusion is consistent with that from EFA ~~method~~ remains uncertain. The  
 420 consistency check is computationally expensive for CFRAM calculation, as ~~the~~ EFA requires high temporal resolution. The  
 present study is based on the Pliocene simulation with the EC-Earth, and the results may be model-dependent. Further work  
 is needed to compare our results with other PlioMIP models.

*Acknowledgements.* This work was supported by the Swedish Research Council VR for the Swedish–French project GIWA, the China Scholarship Council (Grant 201606345010), and the Opening Project of Key Laboratory of Meteorological Disaster of Ministry of Education of Nanjing University of Information Science and Technology (Grant KLME1401). The EC-Earth mid-Pliocene simulation ~~is~~was performed at ECMWF's computing and archive facilities, and the analysis ~~are~~was performed on resources provided by the Swedish National Infrastructure for Computing (SNIC) at Linköping University.

## References

- Alexander, M.A., Bhatt, U.S., Walsh, J.E., Timlin, M.S., Miller, J.S. and Scott, J.D.: The atmospheric response to realistic Arctic sea ice anomalies in an AGCM during winter, *J. Climate*, 17, 890-905, doi:10.1175/1520-0442(2004)017<0890:TARTRA>2.0.CO;2, 2004.
- Alexeev, V.A., Ivanov, V.V., Kwok, R. and Smedsrud, L.H.: North Atlantic warming and declining volume of arctic sea ice, *The Cryosphere Discussions*, 7, 245-265, doi:10.5194/tcd-7-245-2013, 2013.
- Ballantyne, A.P., Axford, Y., Miller, G.H., Otto-Bliesner, B.L., Rosenbloom, N. and White, J.W.: The amplification of Arctic terrestrial surface temperatures by reduced sea-ice extent during the Pliocene, *Palaeogeogr. Palaeoclimatol. Palaeoecol.*, 386, 59-67, doi:10.1016/j.palaeo.2013.05.002, 2013.
- Balsamo, G., Beljaars, A., Scipal, K., Viterbo, P., van den Hurk, B., Hirschi, M. and Betts, A.K.: A revised hydrology for the ECMWF model: Verification from field site to terrestrial water storage and impact in the Integrated Forecast System, *J. Hydrometeorol.*, 10, 623-643, doi:10.1175/2008JHM1068.1, 2009.
- Bintanja, R. and Selten, F.M.: Future increases in Arctic precipitation linked to local evaporation and sea-ice retreat, *Nature*, 509, 479-482, doi:10.1038/nature13259, 2014.
- Bretherton, C.S., Widmann, M., Dymnikov, V.P., Wallace, J.M. and Bladé, I.: The effective number of spatial degrees of freedom of a time-varying field, *J. Climate*, 12, 1990-2009, doi:10.1175/1520-0442(1999)012<1990:TENOSD>2.0.CO;2, 1999.
- Brierley, C. M. and Fedorov, A. V.: Comparing the impacts of Miocene–Pliocene changes in inter-ocean gateways on climate: Central American Seaway, Bering Strait, and Indonesia, *Earth Planet. Sci. Lett.*, 444, 116-130, doi:10.1016/j.epsl.2016.03.010, 2016.
- Brigham-Grette, J., Melles, M., Minyuk, P., Andreev, A., Tarasov, P., DeConto, R. and Haltia, E.: Pliocene warmth, polar amplification, and stepped Pleistocene cooling recorded in NE Arctic Russia. *Science*, 340, 1421, doi:10.1126/science.1233137, 2013.
- Burt, M.A., Randall, D.A. and Branson, M.D.: Dark warming, *J. Climate*, 29, 705-719, doi:10.1175/JCLI-D-15-0147.1, 2016.

- 455 Dowsett, H.J., Robinson, M.M., Haywood, A.M., Hill, D.J., Dolan, A.M., Stoll, D.K., Abe-Ouchi, A., Chandler, M.A.,  
Rosenbloom, N.A., Otto-Bliesner, B.L. and Bragg, F.J.: Assessing confidence in Pliocene sea surface temperatures to  
evaluate predictive models, *Nat. Clim. Change*, 2, 365-371, doi:10.1038/nclimate1455, 2012.
- Dowsett, H., Dolan, A., Rowley, D., Moucha, R., Forte, A. M., Mitrovica, J. X., Pound, M., Salzmann, U., Robinson, M.,  
Chandler, M., Foley, K., and Haywood, A.: The PRISM4 (mid-Piacenzian) paleoenvironmental reconstruction, *Clim. Past*,  
460 12, 1519-1538, doi:10.5194/cp-12-1519-2016, 2016.
- Fedorov, A.V., Dekens, P.S., McCarthy, M., Ravelo, A.C., Barreiro, M., Pacanowski, R.C. and Philander, S.G.: The  
Pliocene paradox (mechanisms for a permanent El Niño), *Science*, 312, 1485-1489, doi:10.1126/science.1122666, 2006.
- Feng, R., Otto-Bliesner, B. L., Fletcher, T. L., Tabor, C. R., Ballantyne, A. P., & Brady, E. C.: Amplified Late Pliocene  
terrestrial warmth in northern high latitudes from greater radiative forcing and closed Arctic Ocean gateways, *Earth Planet.  
Sci. Lett.*, 466, 129-138, doi:10.1016/j.epsl.2017.03.006, 2017.
- 465 Frankignoul, C. and Kestenare, E.: The surface heat flux feedback. Part I: estimates from observations in the Atlantic and the  
North Pacific, *Clim. Dynam.*, 19, 633-647, doi:10.1007/s00382-002-0252-x, 2002.
- Fu, Q. and Liou, K.N.: Parameterization of the radiative properties of cirrus clouds, *J. Atmos. Sci.*, 50, 2008-2025,  
doi:10.1175/1520-0469(1993)050<2008:POTRPO>2.0.CO;2, 1993.
- 470 Gaetani, M., Messori G., Zhang Q., Flamant C., and Pausata F.S.: Understanding the mechanisms behind the northward  
extension of the West African Monsoon during the Mid-Holocene. *J. Climate*, doi:10.1175/JCLI-D-16-0299.1, 2017.
- Gildor, H., Ashkenazy, Y., Tziperman, E. and Lev, I.: The role of sea ice in the temperature-precipitation feedback of glacial  
cycles, *Clim. Dynam.*, 43, 1001-1010, doi:10.1007/s00382-013-1990-7, 2014.
- Graversen, R.G. and Burtu, M.: Arctic amplification enhanced by latent energy transport of atmospheric planetary waves, *Q.  
J. Roy. Meteor. Soc.*, 142, 2046-2054, doi:10.1002/qj.2802, 2016.
- 475 Haywood, A.M., Dowsett, H.J. and Dolan, A.M.: Integrating geological archives and climate models for the mid-Pliocene  
warm period, *Nat. Commun.*, 7, 1-14, doi:10.1038/ncomms10646, 2016a.
- Haywood, A.M., Dowsett, H.J., Dolan, A.M., Chandler, M.A., Hunter, S.J. and Lunt, D.J.: The Pliocene Model  
Intercomparison Project (PlioMIP) Phase 2: scientific objectives and experimental design, *Clim. Past*, 12, 663-675,  
480 doi:10.5194/cp-12-663-2016, 2016b.
- Hazeleger, W., Wang, X., Severijns, C., Ștefănescu, S., Bintanja, R., Sterl, A., Wyser, K., Semmler, T., Yang, S., Van den  
Hurk, B. and Van Noije, T.: EC-Earth V2. 2: description and validation of a new seamless earth system prediction model,  
*Clim. Dynam.*, 39, 2611-2629, doi:10.1007/s00382-011-1228-5, 2012.
- Hill, D.J., Haywood, A.M., Lunt, D.J., Hunter, S.J., Bragg, F.J., Contoux, C., Stepanek, C., Sohl, L., Rosenbloom, N.A.,  
485 Chan, W.L. and Kamae, Y.: Evaluating the dominant components of warming in Pliocene climate simulations, *Clim. Past*,  
10, 79-90, doi:10.5194/cp-10-79-2014, 2014.
- Hu, X., Li, Y., Yang, S., Deng, Y. and Cai, M.: Process-based Decomposition of the Decadal Climate Difference between  
2002-13 and 1984-95, *J. Climate*, 30, 4373-4393, doi:10.1175/JCLI-D-15-0742.1, 2017.

- Kageyama, M., Braconnot, P., Harrison, S. P., Haywood, A. M., Jungclauss, J. H., Otto-Bliesner, B. L., Peterschmitt, J.-Y.,  
490 Abe-Ouchi, A., Albani, S., Bartlein, P. J., Brierley, C., Crucifix, M., Dolan, A., Fernandez-Donado, L., Fischer, H.,  
Hopcroft, P. O., Ivanovic, R. F., Lambert, F., Lunt, D. J., Mahowald, N. M., Peltier, W. R., Phipps, S. J., Roche, D. M.,  
Schmidt, G. A., Tarasov, L., Valdes, P. J., Zhang, Q., and Zhou, T.: The PMIP4 contribution to CMIP6 – Part 1: Overview  
and over-arching analysis plan, *Geosci. Model Dev.*, 11(3), 1033-1057, doi:10.5194/gmd-11-1033-2018, 2018.
- Kim, K.Y., Hamlington, B.D., Na, H. and Kim, J.: Mechanism of seasonal Arctic sea ice evolution and Arctic amplification,  
495 *The Cryosphere*, 10(5), 2191-2202, doi:10.5194/tc-10-2191-2016, 2016.
- Koenigk, T., Brodeau, L., Graverson, R. G., Karlsson, J., Svensson, G., Tjernström, M. and Wyser, K.: Arctic climate change  
in 21st century CMIP5 simulations with EC-Earth, *Climate dynamics*, 40(11-12), 2719-2743, doi: 10.1007/s00382-012-  
1505-y, 2013.
- Kruppen, T., Gerdes, R., Haas, C., Hendricks, S., Herber, A., Selyuzhenok, V., Smedsrud, L. and Spreen, G.: Recent  
500 summer sea ice thickness surveys in Fram Strait and associated ice volume fluxes, *The Cryosphere*, 10, 523-534,  
doi:10.5194/tc-10-523-2016, 2016.
- Lang, A., Yang, S. and Kaas, E.: Sea-ice thickness and recent Arctic warming, *Geophys. Res. Lett.*, 44, 409-418,  
doi:10.1002/2016GL071274, 2017.
- Li, C., Notz, D., Tietsche, S. and Marotzke, J.: The transient versus the equilibrium response of sea ice to global warming,  
505 *J.Climate*, 26, 5624-5636, doi:10.1175/JCLI-D-12-00492.1, 2013.
- Li, G., Ren, B., Zheng, J. and Yang, C.: Net air–sea surface heat flux during 1984–2004 over the North Pacific and North  
Atlantic oceans (10N–50N): annual mean climatology and trend, *Theor. Appl. Climatol.*, 104, 387-401, doi:  
10.1007/s00704-010-0351-2, 2011.
- Liu, Y., Key, J.R., Liu, Z., Wang, X. and Vavrus, S.J.: A cloudier Arctic expected with diminishing sea ice, *Geophys. Res.*  
510 *Lett.*, 39, L05705, doi:10.1029/2012GL051251, 2012.
- Lu, J. and Cai, M.: A new framework for isolating individual feedback processes in coupled general circulation climate  
models. Part I: Formulation, *Clim. Dynam.*, 32, 873–885, doi:10.1007/s00382-008-0425-3, 2009.
- Madec, G.: “NEMO ocean engine”. Note du Pole de mode ’lisation, Institut Pierre-Simon Laplace (IPSL), France, No 27  
ISSN no 1288-1619, 2008.
- 515 Matthiessen, J., Knies, J., Vogt, C. and Stein, R.: Pliocene palaeoceanography of the Arctic Ocean and subarctic seas, *Philos.*  
*Trans. R. Soc. A.*, 367, 21–48, doi: 10.1098/rsta.2008.0203, 2009.
- Muschitiello, F., Zhang, Q., Sundqvist, H.S., Davies, F.J. and Renssen, H.: Arctic climate response to the termination of the  
African Humid Period, *Quat. Sci. Rev.*, 125, 91-97, doi:10.1016/j.quascirev.2015.08.012, 2015.
- Nghiem, S.V., Rigor, I.G., Perovich, D.K., Clemente - Colón, P., Weatherly, J.W. and Neumann, G.: Rapid reduction of  
520 Arctic perennial sea ice, *Geophys. Res. Lett.*, 34, L19504, doi:10.1029/2007GL031138, 2007.
- Otto-Bliesner, B. L., Jahn, A., Feng, R., Brady, E. C., Hu, A. and Löfverström, M.: Amplified North Atlantic warming in  
the late Pliocene by changes in Arctic gateways, *Geophys. Res. Lett.*, 44(2), 957-964, doi:10.1002/2016GL071805, 2017.



- Overland J.E., Wang M., Walsh J.E., Christensen J.H., Kattsov V.M., Champan W.L.: Climate model projections for the Arctic. In: AMAP (2011) Snow, Water, Ice and Permafrost in the Arctic (SWIPA): Climate Change and the Cryosphere. Arctic Monitoring and Assessment Programme (AMAP), Oslo, Norway. Xii, 538 pp, 2011.
- Pausata, F.S., Messori, G. and Zhang, Q.: Impacts of dust reduction on the northward expansion of the African monsoon during the Green Sahara period, *Earth Planet. Sci. Lett.*, 434, 298-307, doi:10.1016/j.epsl.2015.11.049, 2016.
- Pausata, F.S., Emanuel, K.A., Chiacchio, M., Diro, G.T., Zhang, Q., Sushama, L., Stager, J.C. and Donnelly, J.P.: Tropical cyclone activity enhanced by Sahara greening and reduced dust emissions during the African Humid Period, *Proc. Natl. Acad. Sci.*, 114, 6221-6226, doi:10.1073/pnas.1619111114, 2017a.
- Pausata, F.S., Zhang, Q., Muschitiello, F., Lu, Z., Chafik, L., Niedermeyer, E.M., Stager, J.C., Cobb, K.M. and Liu, Z.: Greening of the Sahara suppressed ENSO activity during the mid-Holocene, *Nat. Commun.*, 8, 1-12, doi:10.1038/ncomms16020, 2017b.
- Pithan, F. and Mauritsen, T.: Arctic amplification dominated by temperature feedbacks in contemporary climate models, *Nat. Geosci.*, 7, 181-184, doi:10.1038/ngeo2071, 2014.
- Robinson, M.M., Dowsett, H.J. and Chandler, M.A.: Pliocene role in assessing future climate impacts, *EOS, Trans. Am. Geophys. Union*, 89, 501-502, doi:10.1029/2008EO490001, 2008.
- Serreze, M.C., Barrett, A.P., Stroeve, J.C., Kindig, D.N. and Holland, M.M.: The emergence of surface-based Arctic amplification, *The Cryosphere*, 3, 11-19, doi:10.5194/tc-3-11-2009, 2009.
- Serreze, M.C. and Barry, R.G.: Processes and impacts of Arctic amplification: A research synthesis, *Glob. Planet. Chang.*, 77, 85-96, doi:10.1016/j.gloplacha.2011.03.004, 2011.
- Sévellec, F., Fedorov, A.V. and Liu, W.: Arctic sea-ice decline weakens the Atlantic Meridional Overturning Circulation, *Nat. Clim. Change*, 7, 604-610, doi:10.1038/nclimate3353, 2017.
- Shine, K.P. and Henderson-Sellers, A.: The sensitivity of a thermodynamic sea ice model to changes in surface albedo parameterization. *Journal of Geophysical Research*, 90, 2243–2250, 1985.
- Soden, B. J. and Held, I. M.: An assessment of climate feedbacks in coupled ocean–atmosphere models, *J. Climate*, 19, 3354–3360, doi:10.1175/JCLI3799.1., 2006.
- Song, X. and Zhang, G.J.: Role of climate feedback in El Niño–like SST response to global warming, *J. Climate*, 27, 7301–7318, doi:10.1175/JCLI-D-14-00072.1, 2014.
- Taylor, P.C., Cai, M., Hu, A., Meehl, J., Washington, W. and Zhang, G.J.: A decomposition of feedback contributions to polar warming amplification. *J. Climate*, 26, 7023-7043, doi:10.1175/JCLI-D-12-00696.1, 2013.
- Valcke, S.: OASIS3 user guide (prism\_2-5), PRISM report series, no 2, 6th edn., 2006.
- Vancoppenolle, M., Fichefet T., Goosse H., Bouillon S., Madec G. and Maqueda M. A.: Simulating the mass balance and salinity of Arctic and Antarctic sea ice. 1. Model description and validation, *Ocean Modelling*, 27, 33-53, doi:10.1016/j.oceanmod.2008.10.005., 2009.

- Venegas, S. A., Mysak, L. A. and Straub, D. N.: Atmosphere–ocean coupled variability in the South Atlantic. *J. Climate*, 10(11), 2904-2920, doi:10.1175/1520-0442(1997)010<2904:AOCVIT>2.0.CO;2, 1997.
- Vihma, T.: Effects of Arctic sea ice decline on weather and climate: a review. *Surv. Geophys.*, 35, 1175-1214, doi:10.1007/s10712-014-9284-0, 2014.
- 560 Wara, M.W., Ravelo, A.C. and Delaney, M.L.: Permanent El Niño-like conditions during the Pliocene warm period. *Science*, 309, 758-761, doi:10.1126/science.1112596, 2005.
- Wetherald, R. T. and Manabe S.: Cloud feedback processes in a general circulation model. *J. Atmos. Sci.*, 45, 1397–1416, doi:10.1175/1520-0469(1988)045<1397:CFPIAG>2.0.CO;2., 1988.
- Winton, M.: Sea ice–albedo feedback and nonlinear Arctic climate change. Arctic sea ice decline: Observations, projections, mechanisms, and implications, 111-131, doi:10.1029/180GM09, 2008.
- 565 Zheng, J., Ren, B., Li, G. and Yang, C.: Seasonal dependence of local air-sea interaction over the tropical Western Pacific warm pool. *J. Trop. Meteorol.*, 20(4), 360-367, doi:10.16555/j.1006-8775.2014.04.009, 2014.

570

575

580

585

590

**Table 1.** The spatial standard deviation of SIC anomalies  $\sigma_{\text{SIC}}$  and net shortwave radiation anomalies due to albedo effect  $\sigma_{\text{SW-albedo}}$  ( $\text{Wm}^{-2}$ ) over the Arctic Ocean.  $r_{\text{SW-albedo}}$  is the correlation coefficient between SIC and shortwave radiation anomalies. Those significant at a 99% confidence level are bolded.

	Jan	Feb	Mar	Apr	May	Jun	Jul	Aug	Sep	Oct	Nov	Dec
$\sigma_{\text{SIC}}$	<u>0.4425</u>	<u>0.4426</u>	<u>0.4426</u>	<u>0.4326</u>	<u>0.4325</u>	<u>0.3923</u>	<u>0.3423</u>	<u>0.3620</u>	<u>0.3919</u>	<u>0.3825</u>	<u>0.4025</u>	<u>0.4325</u>
$\sigma_{\text{SW-albedo}}$	<u>0.0301</u>	<u>1.550</u>	<u>11.095</u>	<u>42.792</u>	<u>88.435</u>	<u>80.374</u>	<u>41.882</u>	<u>29.851</u>	<u>15.066</u>	<u>3.592</u>	<u>0.2021</u>	0
		<u>75</u>	<u>.81</u>	<u>5.34</u>	<u>2.45</u>	<u>8.79</u>	<u>6.28</u>	<u>2.39</u>	<u>.85</u>	<u>16</u>		
$r_{\text{SW-albedo}}$	<u>-</u>	<u>-</u>	<u>-</u>	<u>-</u>	<u>-</u>	<u>-</u>	<u>-</u>	<u>-</u>	<u>-</u>	<u>-</u>	<u>-</u>	/
	<u>0.2522</u>	<u>0.4337</u>	<u>0.7563</u>	<u>0.8877</u>	<u>0.9080</u>	<u>0.9185</u>	<u>0.9085</u>	<u>0.9383</u>	<u>0.8857</u>	<u>0.5053</u>	<u>0.2511</u>	

595

**Table 2.** The spatial standard deviation of shortwave and longwave radiation anomalies due to cloud change ( $\sigma_{\text{SW-cloud}}$ ,  $\sigma_{\text{LW-cloud}}$ ) ( $\text{Wm}^{-2}$ ) and water vapour change ( $\sigma_{\text{SW-WV}}$ ,  $\sigma_{\text{LW-WV}}$ ) ( $\text{Wm}^{-2}$ ) over the Arctic Ocean.  $r_{\text{SW-cloud}}$ ,  $r_{\text{LW-cloud}}$ ,  $r_{\text{SW-WV}}$  and  $r_{\text{LW-WV}}$  are correlation coefficients between SIC and shortwave and longwave radiation anomalies due to cloud and water change, respectively. Those significant at a 99% confidence level are bolded. Here, a the cloud and water vapour change is specified as the part caused by sea -ice decrease.

	<u>Annual</u>	<u>Jan</u>	<u>Feb</u>	<u>Mar</u>	<u>Apr</u>	<u>May</u>	<u>Jun</u>	<u>Jul</u>	<u>Aug</u>	<u>Sep</u>	<u>Oct</u>	<u>Nov</u>	<u>Dec</u>
<u><math>\sigma_{\text{SW-cloud}}</math></u>	<u>4.76</u>	<u>0.01</u>	<u>0.16</u>	<u>1.11</u>	<u>3.86</u>	<u>5.97</u>	<u>11.71</u>	<u>19.61</u>	<u>13.86</u>	<u>3.21</u>	<u>0.50</u>	<u>0.04</u>	<u>0</u>
<u><math>r_{\text{SW-cloud}}</math></u>	<u>0.18</u>	<u>0.14</u>	<u>0.22</u>	<u>0.36</u>	<u>0.36</u>	<u>0.16</u>	<u>0.01</u>	<u>0.05</u>	<u>0.24</u>	<u>0.26</u>	<u>0.25</u>	<u>0.32</u>	<u>/</u>
<u><math>\sigma_{\text{LW-cloud}}</math></u>	<u>8.02</u>	<u>9.13</u>	<u>9.29</u>	<u>8.25</u>	<u>7.64</u>	<u>10.20</u>	<u>11.91</u>	<u>15.11</u>	<u>13.56</u>	<u>11.96</u>	<u>10.01</u>	<u>10.18</u>	<u>9.86</u>
<u><math>r_{\text{LW-cloud}}</math></u>	<u>-0.46</u>	<u>-0.59</u>	<u>-0.56</u>	<u>-0.56</u>	<u>-0.51</u>	<u>-0.36</u>	<u>0.06</u>	<u>0.04</u>	<u>-0.23</u>	<u>-0.54</u>	<u>-0.41</u>	<u>-0.60</u>	<u>-0.56</u>
<u><math>\sigma_{\text{SW-WV}}</math></u>	<u>0.29</u>	<u>0.001</u>	<u>0.03</u>	<u>0.14</u>	<u>0.40</u>	<u>0.59</u>	<u>0.85</u>	<u>0.85</u>	<u>0.63</u>	<u>0.33</u>	<u>0.09</u>	<u>0.01</u>	<u>0</u>
<u><math>r_{\text{SW-WV}}</math></u>	<u>-0.02</u>	<u>-0.05</u>	<u>0.02</u>	<u>0.06</u>	<u>0.05</u>	<u>0.02</u>	<u>0.11</u>	<u>-0.07</u>	<u>-0.57</u>	<u>-0.62</u>	<u>-0.43</u>	<u>-0.22</u>	<u>/</u>
<u><math>\sigma_{\text{LW-WV}}</math></u>	<u>2.27</u>	<u>3.45</u>	<u>3.53</u>	<u>3.11</u>	<u>2.84</u>	<u>2.57</u>	<u>2.72</u>	<u>2.15</u>	<u>1.73</u>	<u>1.77</u>	<u>2.31</u>	<u>2.89</u>	<u>3.54</u>
<u><math>r_{\text{LW-WV}}</math></u>	<u>-0.56</u>	<u>-0.45</u>	<u>-0.43</u>	<u>-0.50</u>	<u>-0.58</u>	<u>-0.57</u>	<u>-0.46</u>	<u>-0.13</u>	<u>0.38</u>	<u>0.13</u>	<u>-0.36</u>	<u>-0.58</u>	<u>-0.49</u>

600

	Annual	Jan	Feb	Mar	Apr	May	Jun	Jul	Aug	Sep	Oct	Nov	Dec
$\sigma_{SW-cloud}$	4.8676	0.01	0.16	1.2011	4.5638	6.8459	12.5311	19.1461	14.4513	4.1632	0.6550	0.04	0
$r_{SW-cloud}$	0.3118	0.1514	0.2722	0.4136	0.4236	0.2916	0.1901	0.2105	0.3524	0.4026	0.3725	0.32	/
$\sigma_{LW-cloud}$	8.2502	8.8991	9.1929	8.1325	7.9664	10.7320	11.8191	14.0615	13.5556	13.6411	11.3110	10.3118	9.8386
$r_{LW-cloud}$	-0.5246	-0.5859	-0.5956	-0.5856	-0.5551	-0.4536	-0.0906	-0.0704	-0.3323	-0.6254	-0.5241	-0.6460	-0.5856
$\sigma_{SW-WV}$	0.2729	0.001	0.03	0.14	0.3840	0.5759	0.7985	0.7785	0.5663	0.2833	0.0809	0.01	0
$r_{SW-WV}$	-0.0702	-0.0805	-0.0302	0.0106	-0.0105	-0.0602	0.0611	-0.0807	-0.4957	-0.5662	-0.4443	-0.2422	/
$\sigma_{LW-WV}$	2.2327	3.4045	3.4653	3.0711	2.8084	2.5157	2.5372	1.9221	1.5573	1.5877	2.2131	2.9689	3.6154
$r_{LW-WV}$	-0.6256	-0.5045	-0.4843	-0.5650	-0.6258	-0.6057	-0.4846	-0.1213	0.3338	-0.0613	-0.5236	-0.6758	-0.5749

605

610

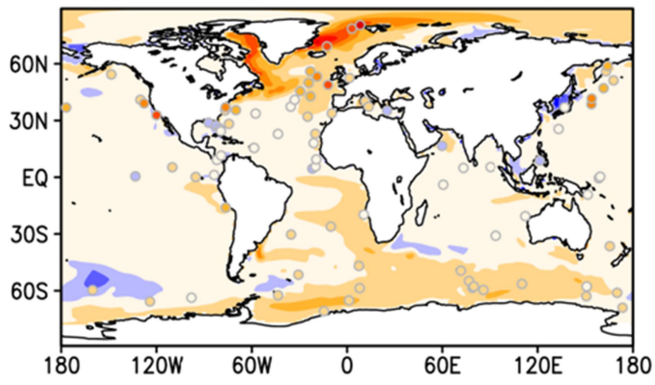
**Table 3.** The spatial standard deviation of sensible and latent heat flux anomalies  $\sigma_{SH}$ ,  $\sigma_{LH}$  ( $Wm^{-2}$ ) over the Arctic Ocean.  $r_{SH}$  and  $r_{LH}$  are correlation coefficients between SIC and sensible and latent heat flux anomalies, respectively. Those significant at a 99% confidence level are bolded.

	Jan	Feb	Mar	Apr	May	Jun	Jul	Aug	Sep	Oct	Nov	Dec
$\sigma_{SH}$	28.53	29.44	21.64	12.87	7.94	9.46	9.55	2.63	2.11	7.02	31.11	26.80
$r_{SH}$	<b>0.57</b>	<b>0.64</b>	<b>0.67</b>	<b>0.66</b>	<b>0.76</b>	0.26	<u>-0.36</u>	0.03	<b>0.65</b>	<b>0.80</b>	<b>0.71</b>	<b>0.56</b>
$\sigma_{LH}$	18.70	19.00	14.75	9.46	5.64	5.84	8.75	1.93	1.69	5.77	19.87	17.44
$r_{LH}$	<b>0.74</b>	<b>0.77</b>	<b>0.78</b>	<b>0.76</b>	<b>0.71</b>	0.14	<u>-0.42</u>	<u>-0.37</u>	<b>0.69</b>	<b>0.90</b>	<b>0.79</b>	<b>0.72</b>

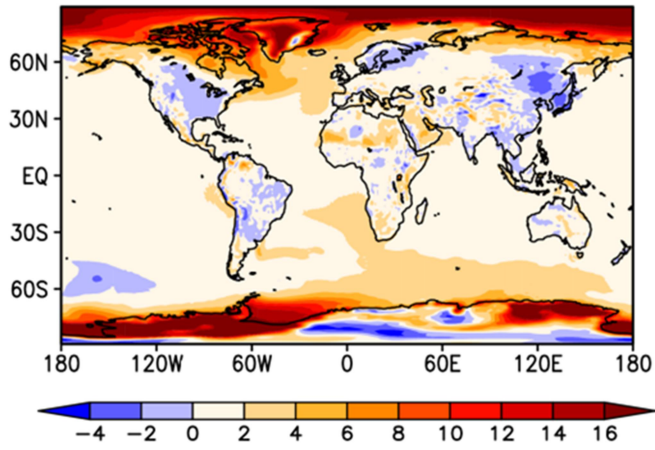
**Table 4.** The response coefficients ( $Wm^{-2}$ ) of radiation and turbulent heat fluxes to the albedo and insulation effects of sea ice. Those significant at a 99% confidence level are bolded.

$\lambda$ ( $Wm^{-2}$ )	flux	Ann	Jan	Feb	Mar	Apr	May	Jun	Jul	Aug	Sep	Oct	Nov	Dec
albedo	SW	-	-	-	-	-	-	-	-	-	-	-	-	-
		<u>46.5</u>	0.0	<u>1.71</u>	<u>18.9</u>	<u>87.2</u>	<u>188.1</u>	<u>186.0</u>	<u>109.7</u>	<u>-77.5</u>	<u>34.4</u>	<u>4.75</u>	<u>-0.1</u>	0
		<b>43.0</b>			<b>13.8</b>	<b>75.0</b>	<b>169.2</b>	<b>178.3</b>	<b>97.0</b>	<b>52.0</b>	<b>20.2</b>			
	cloud	<u>4.32</u>	0.0	0.1	<u>1.10</u>	<u>4.43</u>	<u>4.62</u>	<u>6.10</u>	<u>11.3</u>	<u>13.79</u>	<u>4.23</u>	<u>0.64</u>	0.0	0
	SW													
insulation	WV	<u>-0.10</u>	0.0	0.0	0.0	0.0	<u>-0.10</u>	<u>0.12</u>	<u>-0.2</u>	<u>-1.07</u>	<u>0.45</u>	<u>-0.1</u>	0.0	0
	cloud	-	-	-	-	-	-	-	-	-	-	-	-	-
		<u>12.6</u>	<u>11.9</u>	<u>12.2</u>	<u>10.84</u>	<u>10.0</u>	<u>-11.4</u>	<u>-21.7</u>	<u>-</u>	<u>-12.2</u>	<u>21.3</u>	<u>15.2</u>	<u>16.4</u>	<u>-</u>
	LW	<b>11.1</b>	<b>12.1</b>	<b>11.7</b>		<b>8.9</b>	<b>8.6</b>		<b>2.81</b>	<b>9.0</b>	<b>17.6</b>	<b>11.6</b>	<b>15.8</b>	<b>13.60</b>
	WV	<u>-4.0</u>	<u>-</u>	<u>-</u>	<u>-3.95</u>	<u>-4.0</u>	<u>-3.64</u>	<u>-3.12</u>	<u>-0.79</u>	<u>1.49</u>	<u>-0.36</u>	<u>-</u>	<u>-5.0</u>	<u>-</u>
		<b>3.9</b>	<b>3.95</b>	<b>3.84</b>		<b>3.7</b>					<b>2.30</b>	<b>4.4</b>	<b>4.81</b>	
	SH	35.3	53.4	59.0	46.4	29.6	24.2	10.4	<u>-13.8</u>	0.4	7.1	22.3	79.2	54.0
	LH	27.7	45.3	46.0	36.6	25.0	16.1	3.5	<u>-15.0</u>	<u>-3.6</u>	6.0	20.5	56.7	45.7

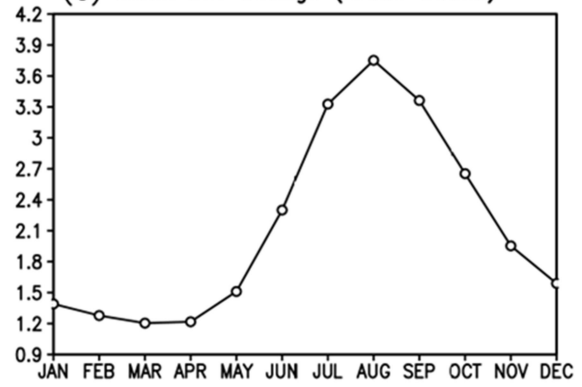
(a) SST change (Pliocene–Preindustrial)



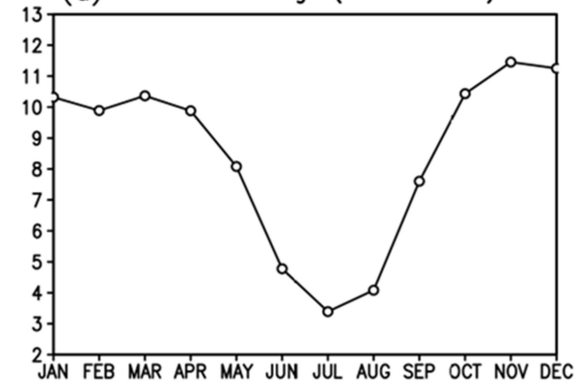
(b) SAT change (Pliocene–Preindustrial)

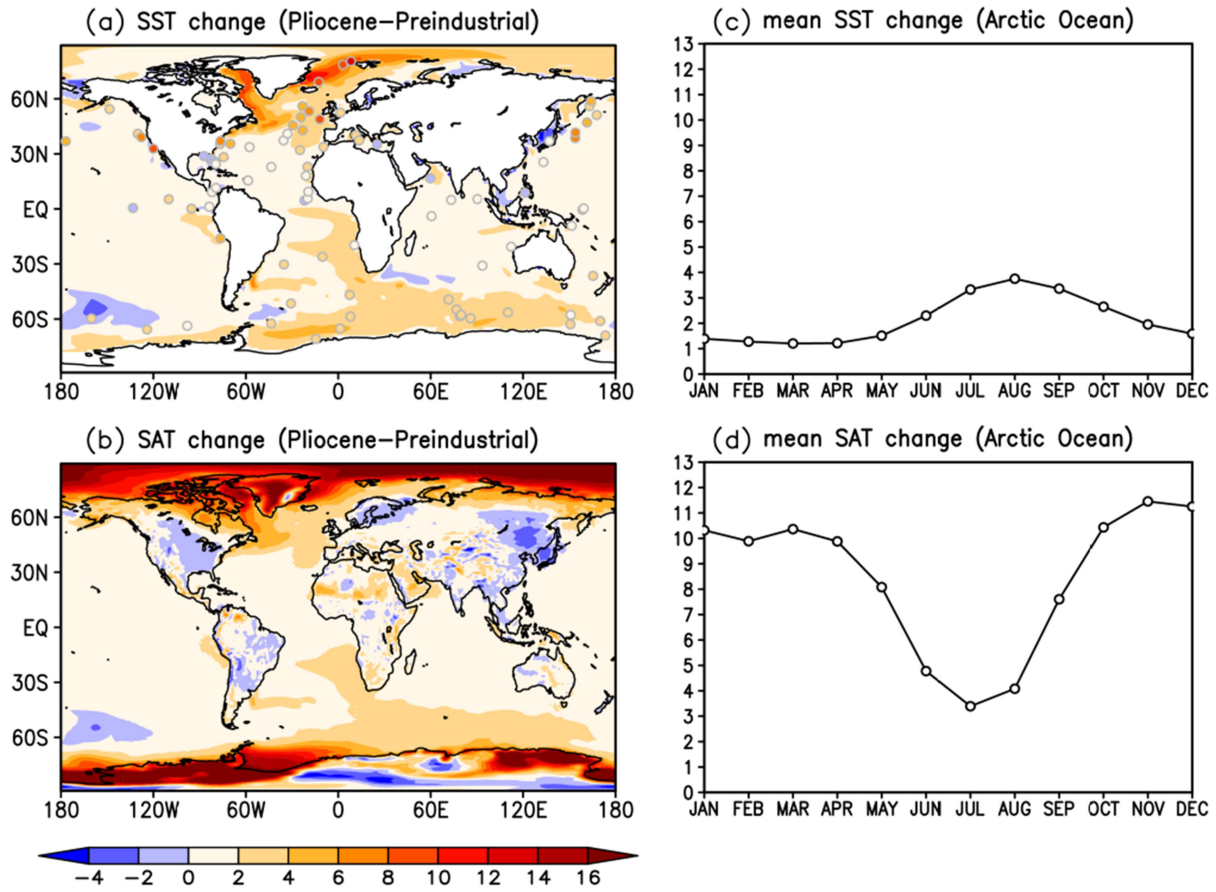


(c) mean SST change (Arctic Ocean)



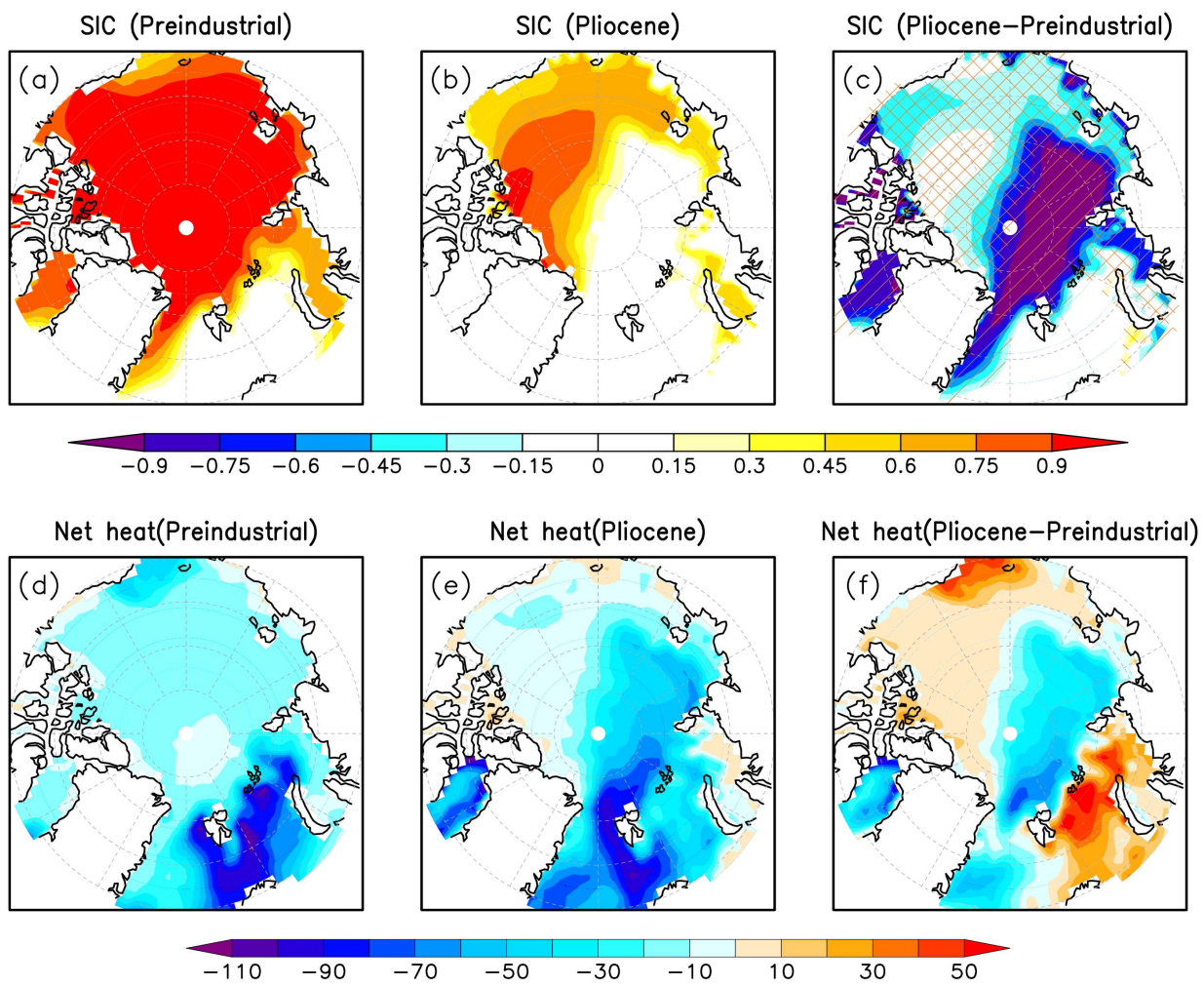
(d) mean SAT change (Arctic Ocean)

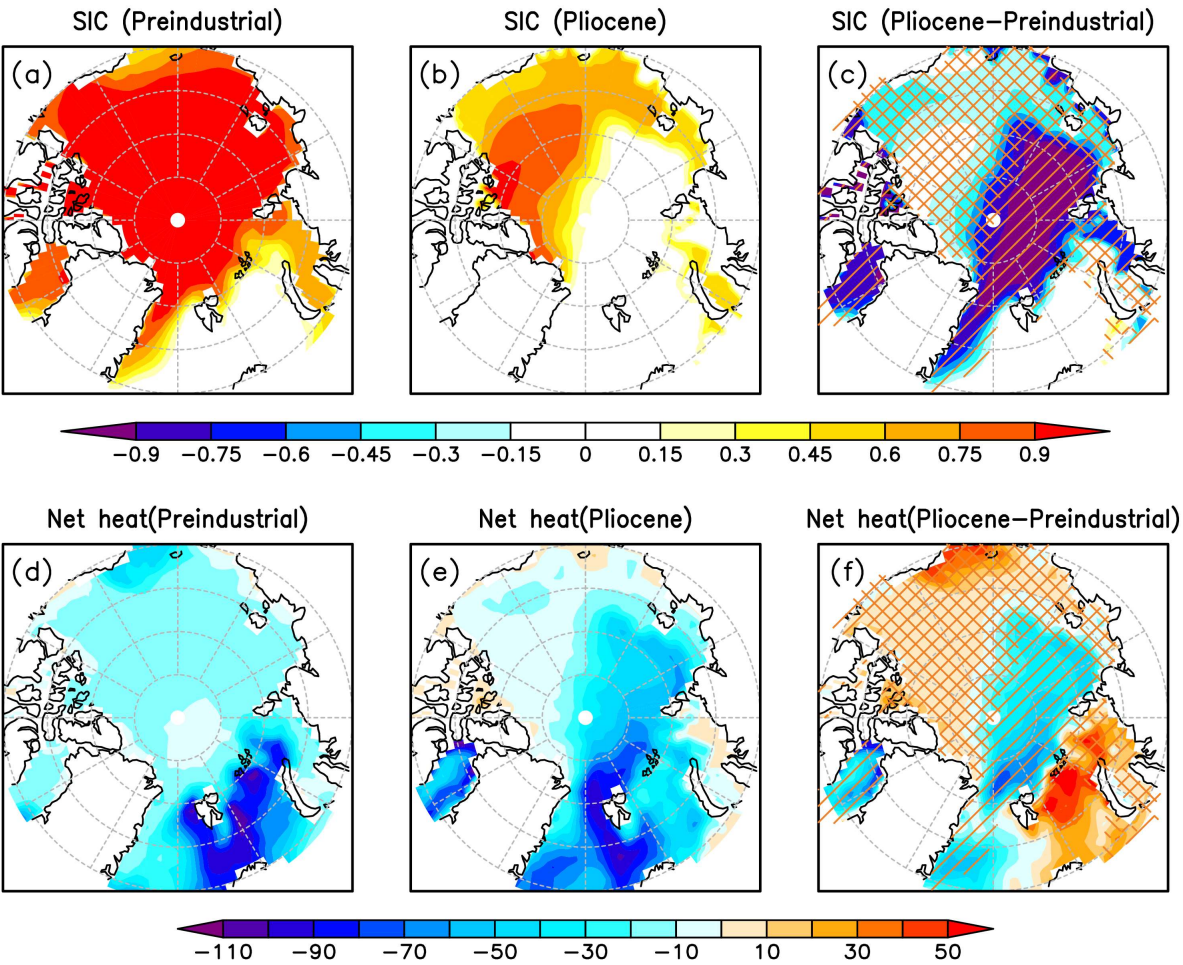




625 **Figure 1.** The annual mean warming (K) for (a) sea surface temperature (SST) and (b) surface air temperature (SAT), and seasonal warming (K) averaged over the Arctic Ocean for (c) SST, and (d) SAT between the Pliocene and preindustrial simulations. The shaded circles in (a) represent the annual mean SST anomalies at 95% confidence-assessed marine sites from the Deep Sea Drilling Project (DSDP) and Ocean Drilling Program (ODP).



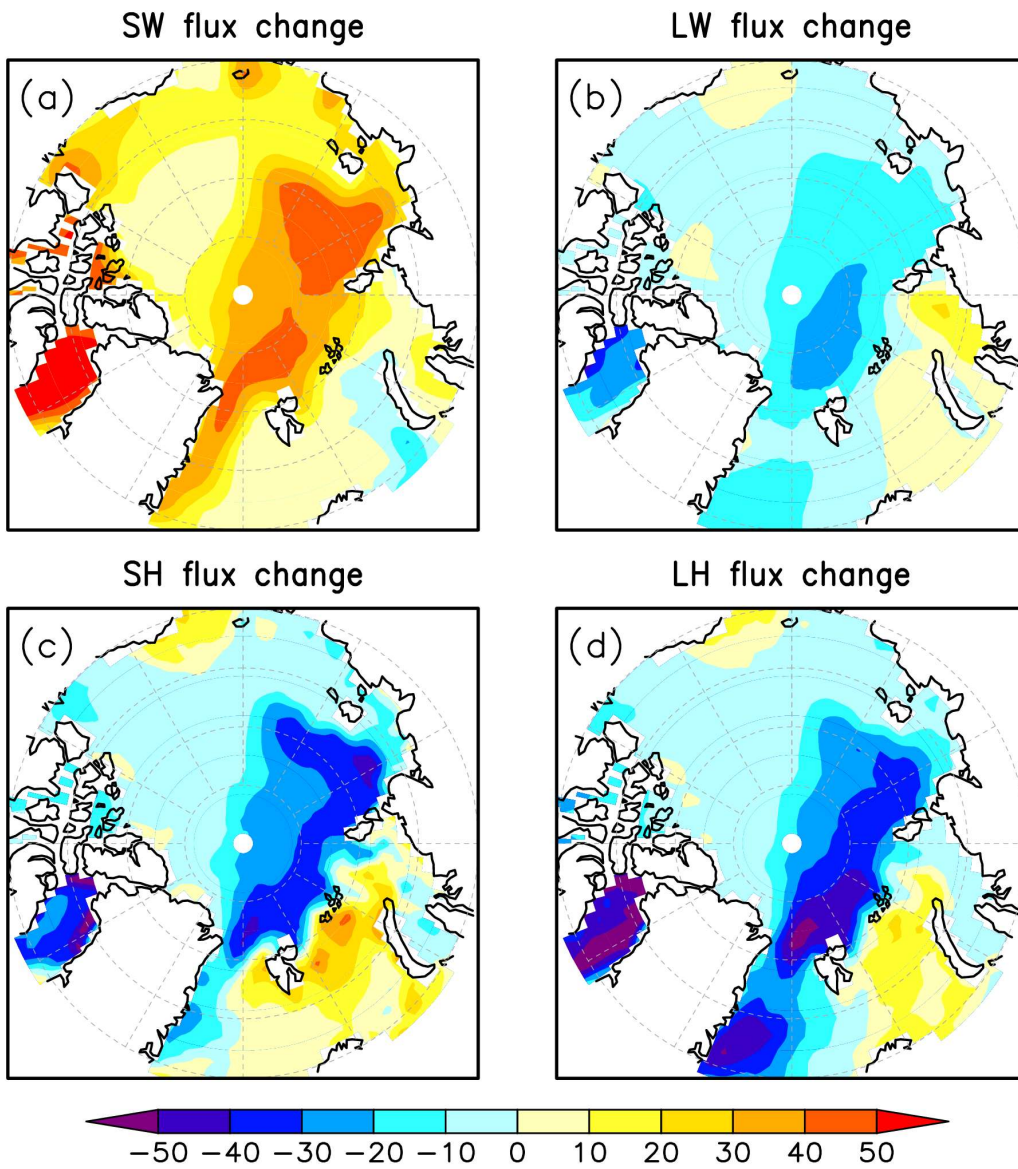




635

**Figure 2.** Spatial distributions of the annual mean sea -ice concentration (SIC) and ~~air-sea interface~~ net heat flux at the surface of ice and ocean ( $\text{Wm}^{-2}$ , positive downward) over the Arctic Ocean. (a) SIC in the preindustrial period, (b) SIC in the Pliocene, (c) the Pliocene SIC change with respect to the preindustrial period, (d) net heat flux in the preindustrial period, (e) net heat flux in the Pliocene, and (f) the Pliocene net heat flux change with respect to the preindustrial period. The diagonal stripe in (c) represents the regions from ice-covered to ice-free, and the diagonal crosshatch represents the regions from ice-covered to ice-covered.

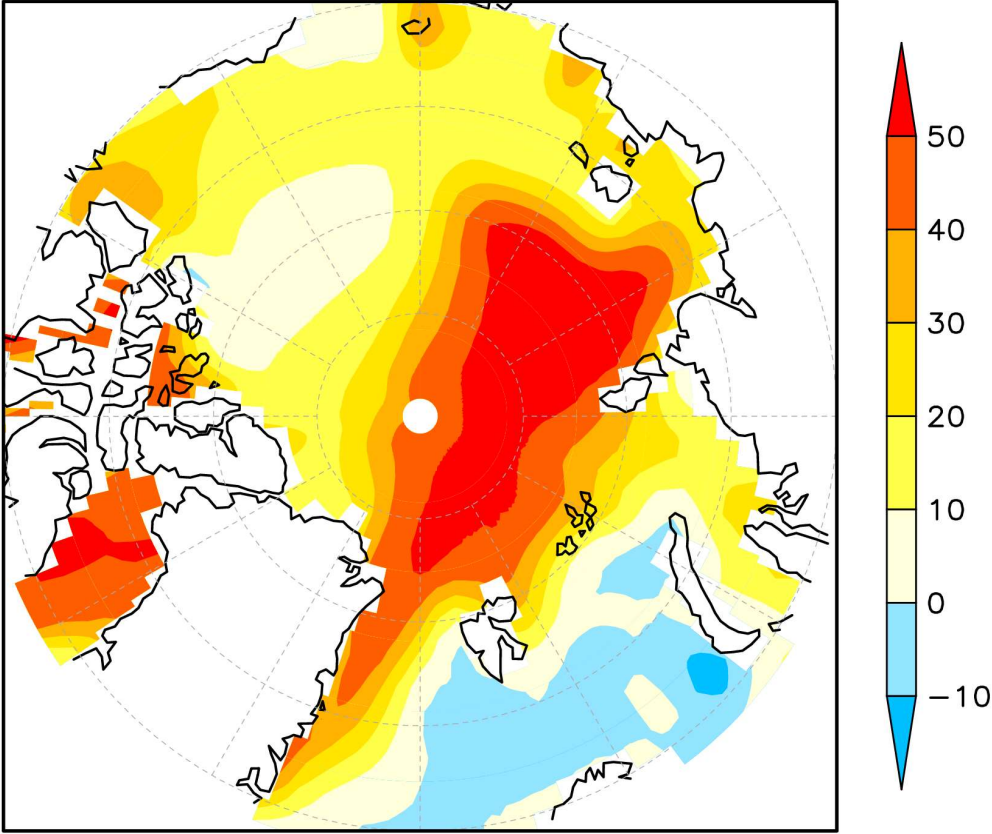
640



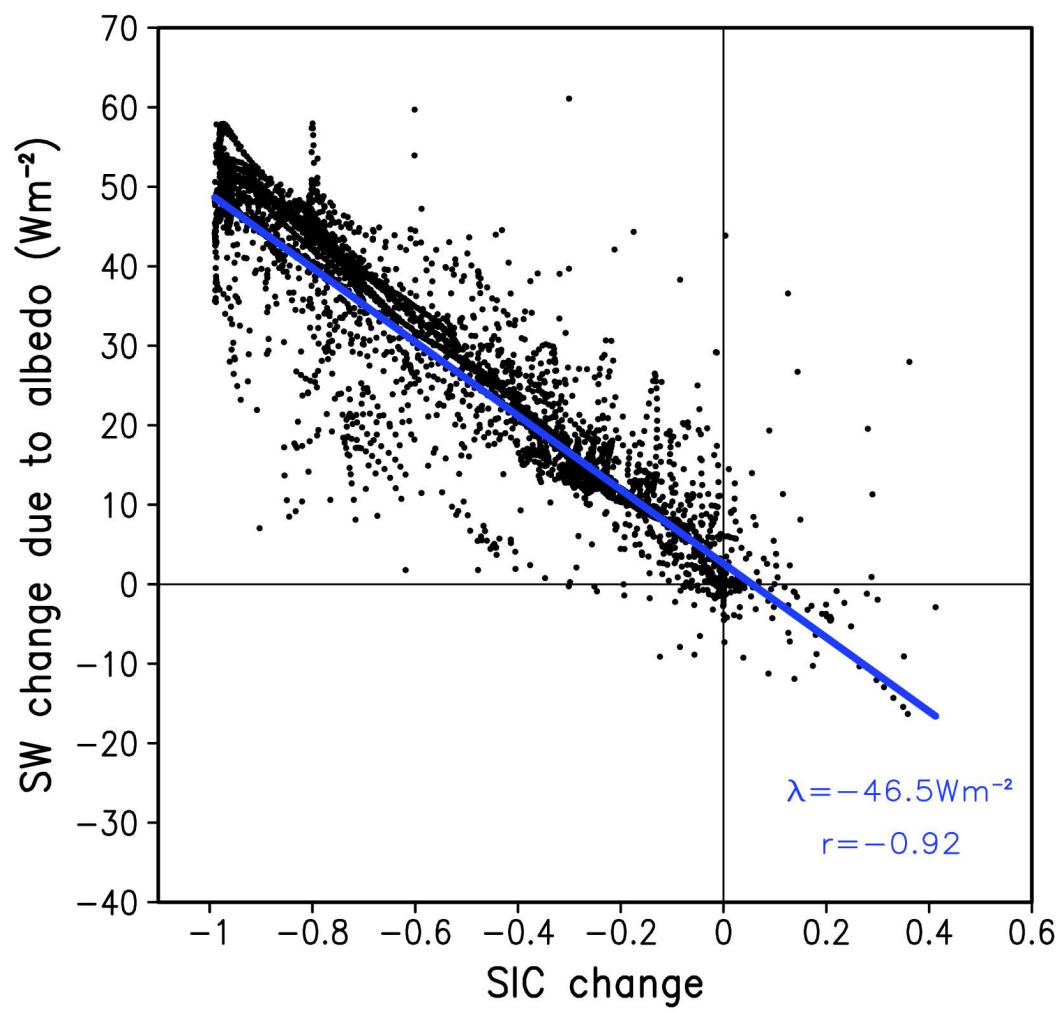
645 | **Figure 3.** Spatial distributions of the Pliocene annual mean heat flux change ( $\text{Wm}^{-2}$ , positive downward) with respect to the preindustrial period over the Arctic Ocean. (a) net shortwave radiation-flux, (b) net longwave radiation flux, (c) sensible heat flux, and (d) latent heat flux.

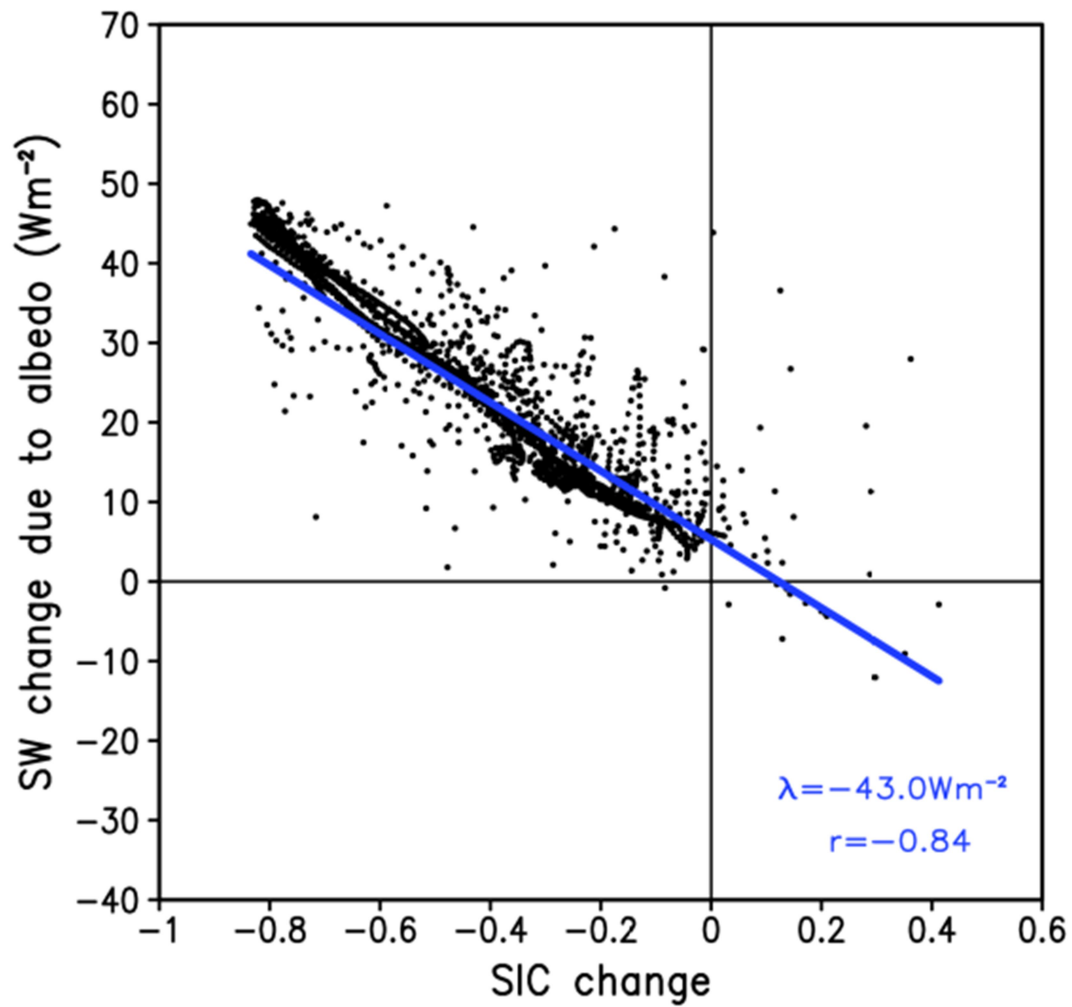


Mean annual SW change due to albedo effect

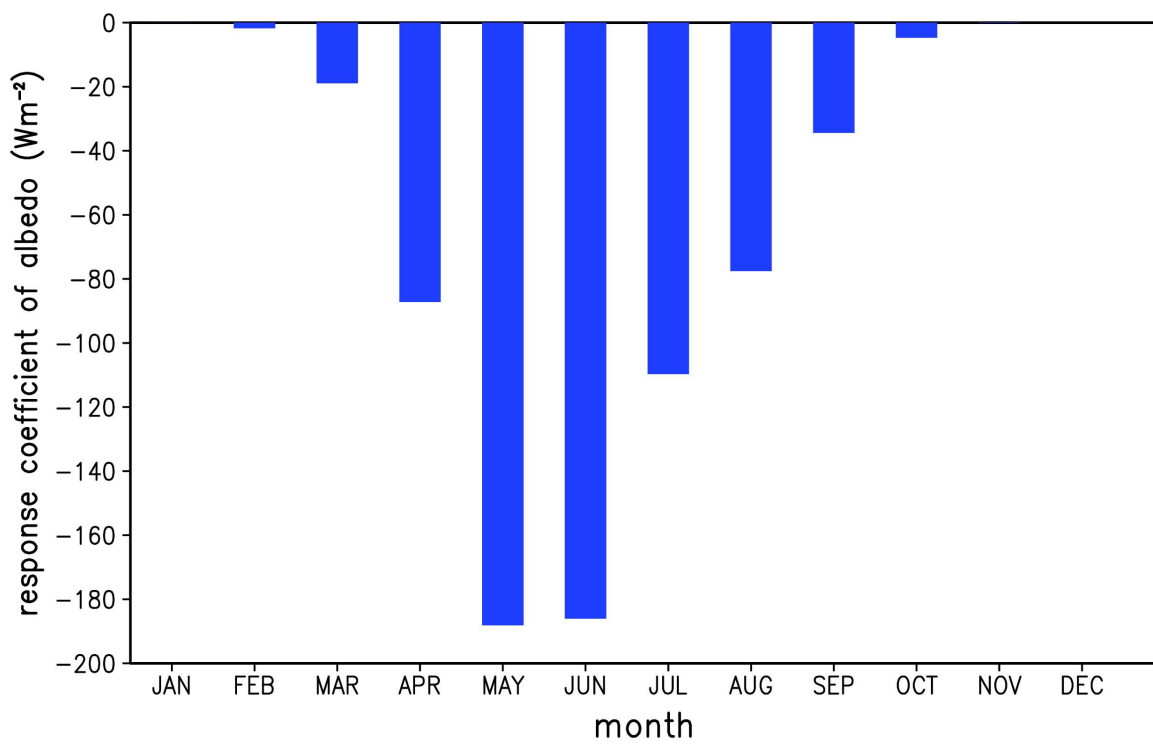


655 | **Figure 4.** Spatial distributions of the Pliocene annual mean net shortwave radiation-flux change ( $\text{Wm}^{-2}$ , positive downward) at the surface over the Arctic Ocean caused by albedo effect of sea -ice change with respect to the preindustrial period.





**Figure 5.** The annual mean net shortwave radiation-flux change ( $\text{Wm}^{-2}$ , positive downward) caused by the albedo effect of sea -ice change averaged over the Arctic Ocean as a function of SIC change. All the change areis with respect to the preindustrial period, and each dot represents one grid point value over the Arctic Ocean.





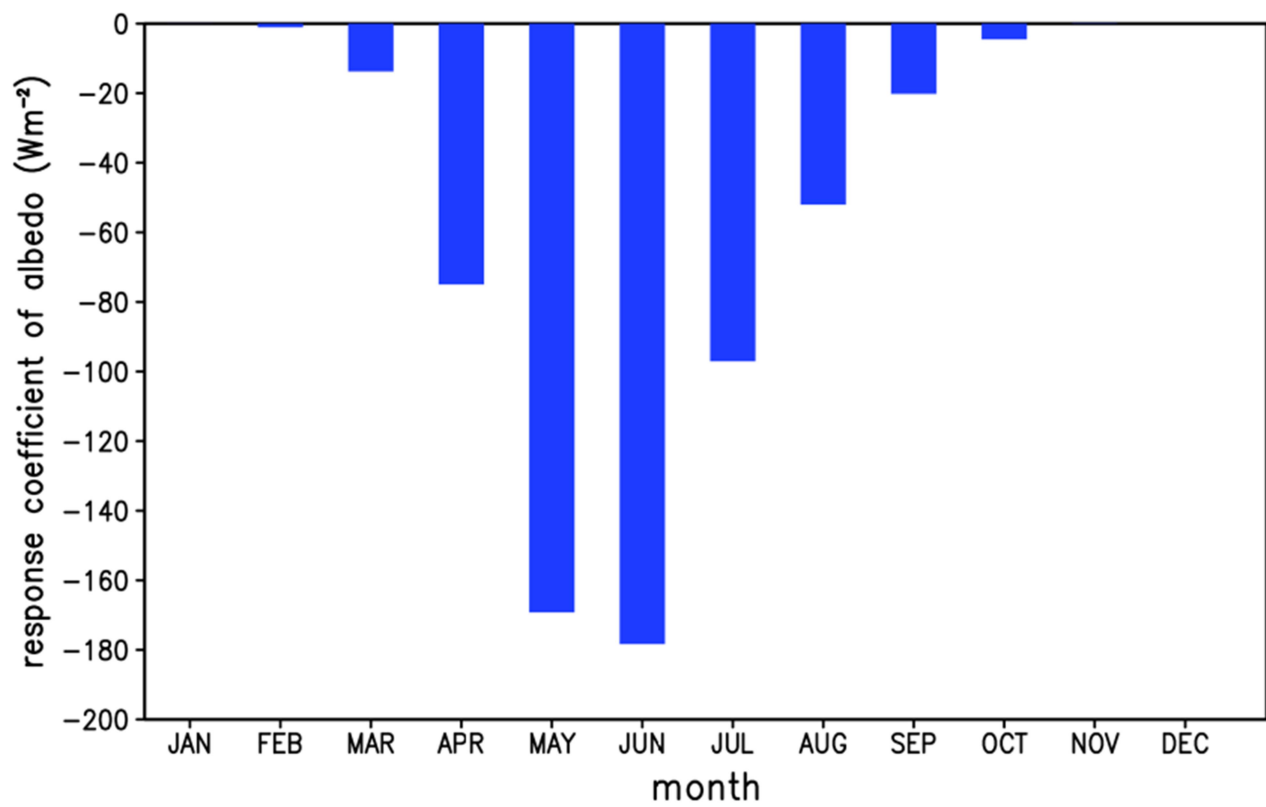
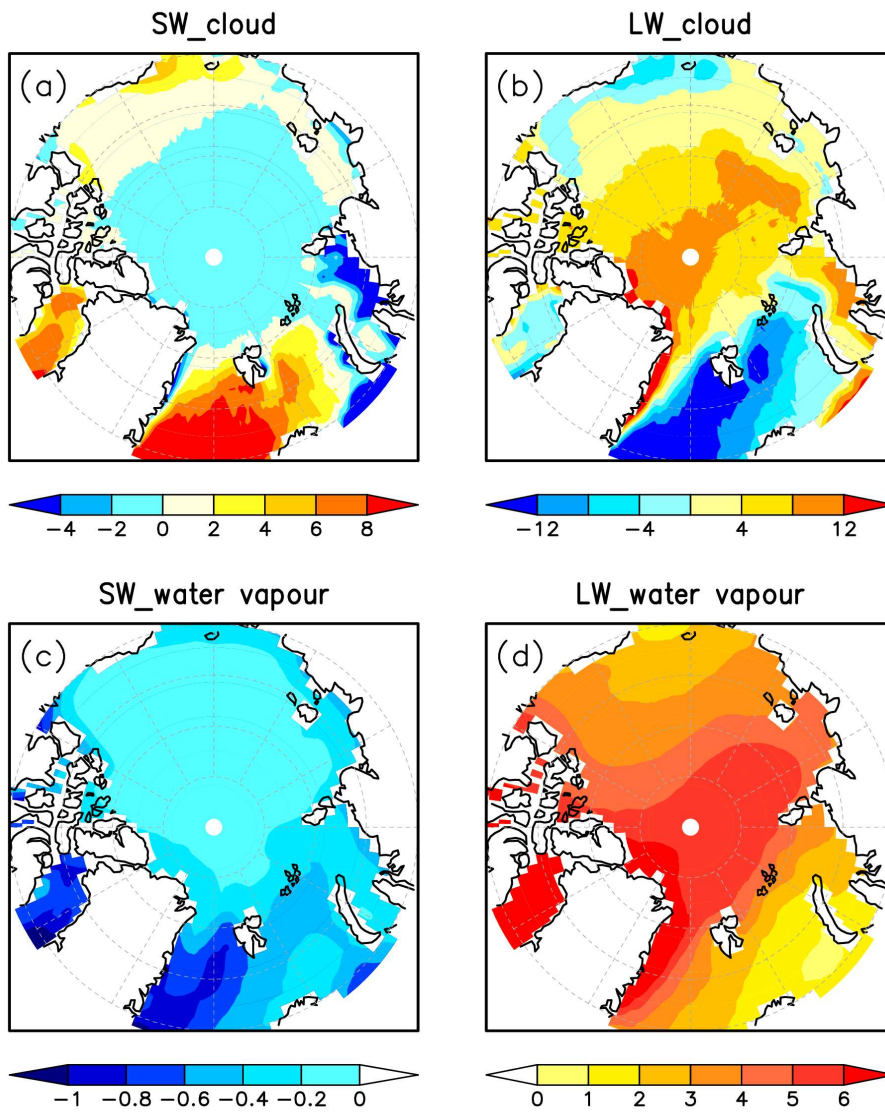
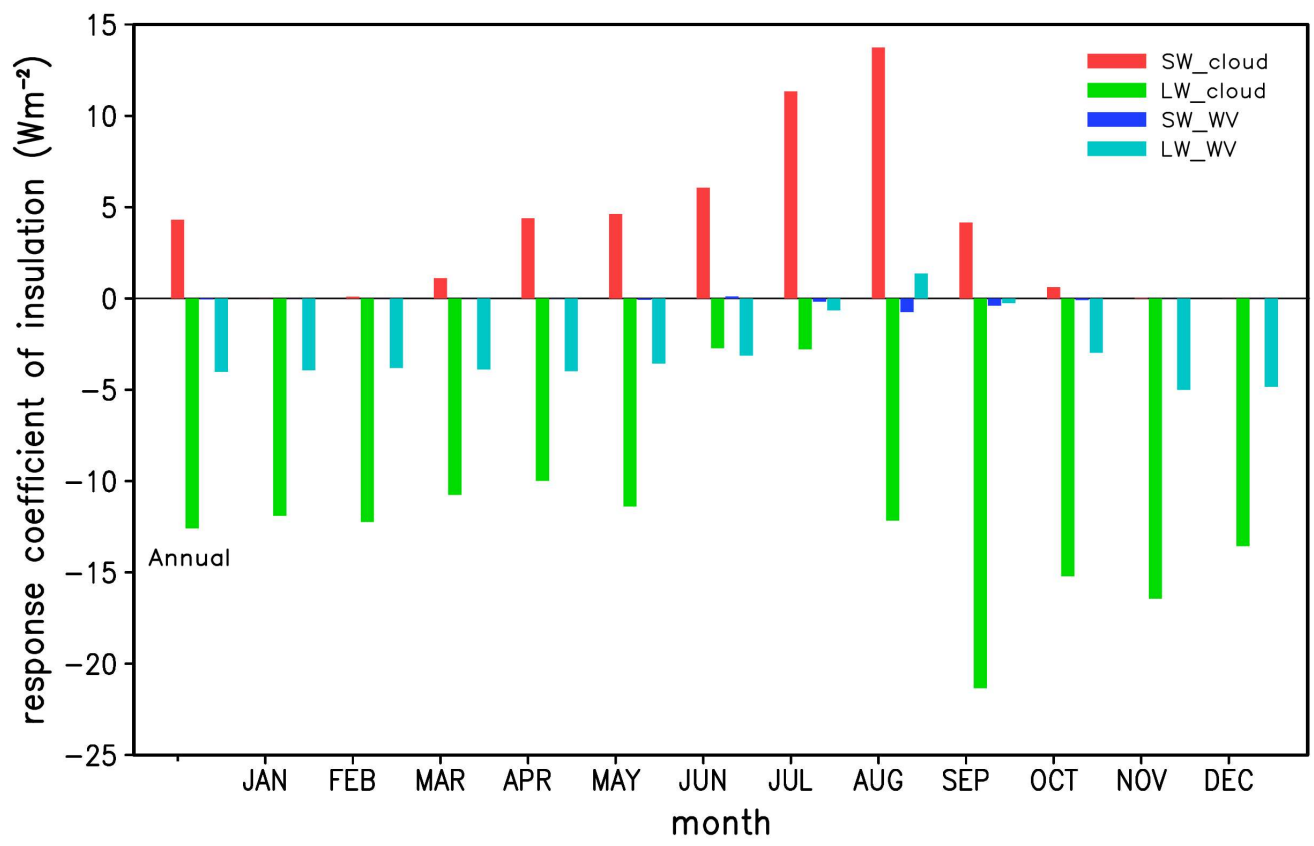
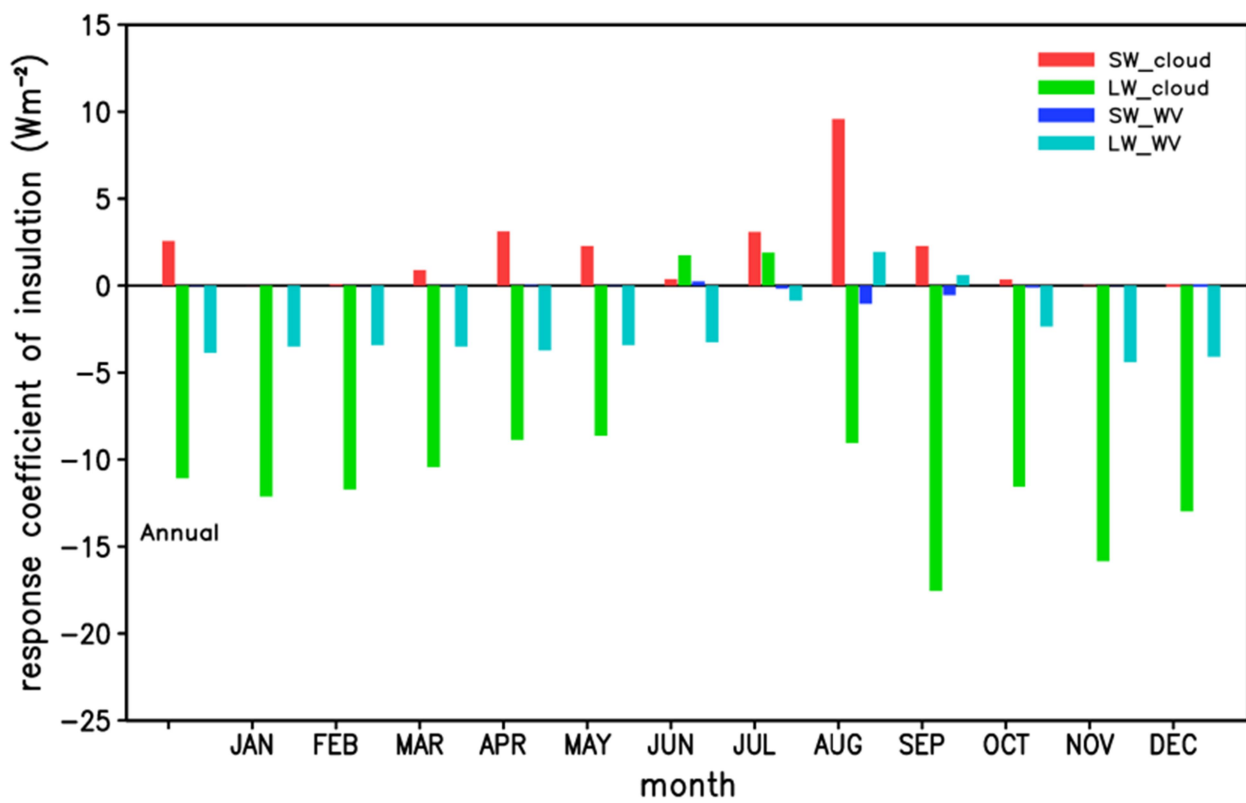


Figure 6. The monthly response coefficients ( $\text{Wm}^{-2}$ ) of net shortwave ~~radiation~~-flux to the albedo effect of sea -ice.



**Figure 7.** Spatial distributions of the Pliocene annual mean radiation fluxes change ( $\text{Wm}^{-2}$ , positive downward) with respect to the preindustrial period over the Arctic Ocean. (a) shortwave radiation due to cloud change, (b) longwave radiation due to cloud change, (c) shortwave radiation due to water vapour change, (d) longwave radiation due to water vapour change. Here ~~the~~<sub>-</sub> cloud and water vapour change is specified as the value before removing the part caused by sea-ice decrease remote effects of clouds and water vapour.





**Figure 8.** The annual and monthly response coefficients ( $\text{Wm}^{-2}$ ) of net shortwave and longwave radiation flux ~~caused-by~~related to cloud and water vapour change to the insulation effect of sea ~~-ice~~. Here, the cloud and water vapour change is specified as the part ~~caused~~byrelated to sea ~~-ice~~ decrease.

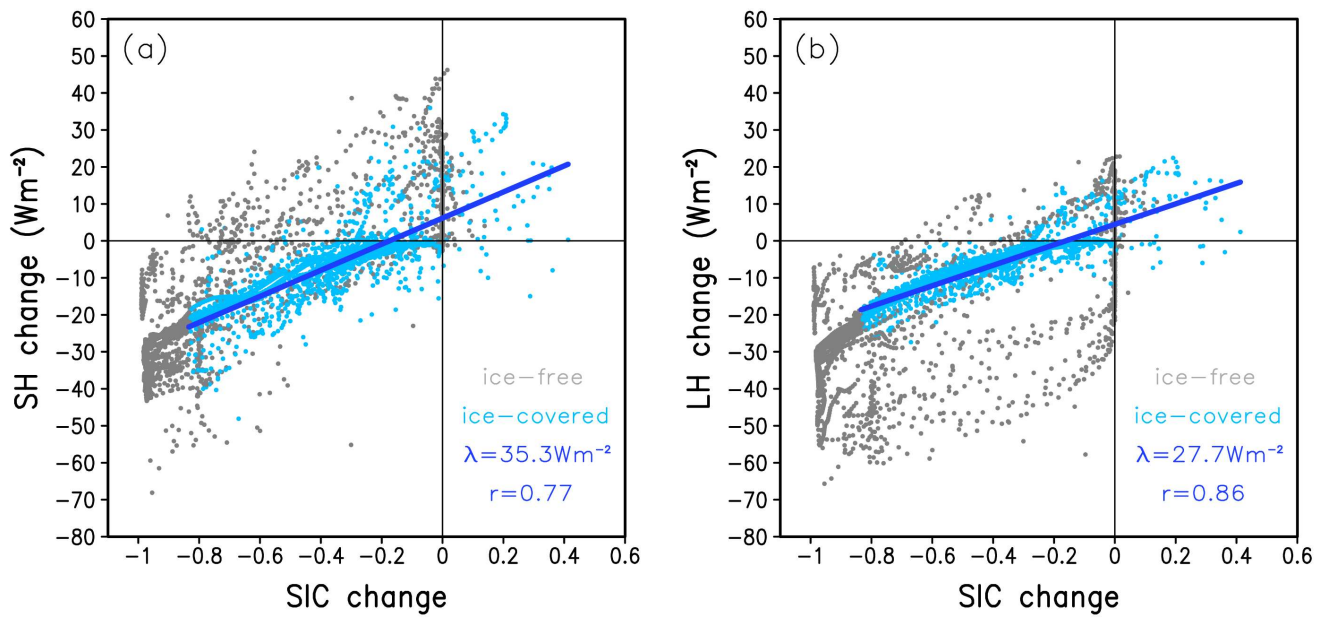
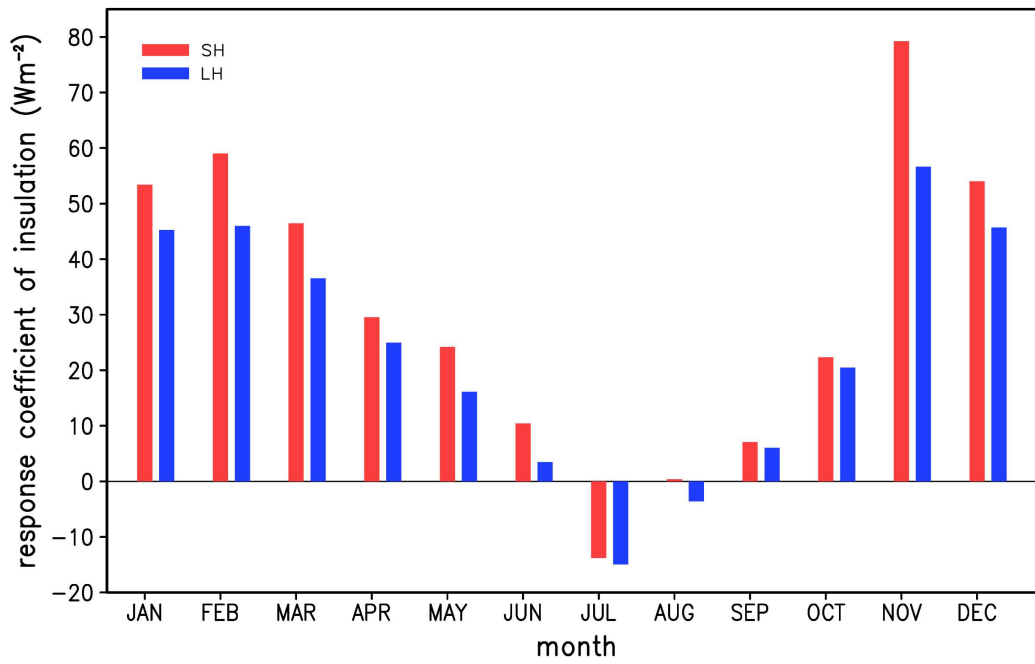


**Figure 9.** The annual mean sensible and latent heat flux change ( $\text{Wm}^{-2}$ , positive downward) caused by related to insulation effect of sea - ice change averaged over the Arctic Ocean as a function of SIC change. All the change Pliocene changes shown are with respect computed relative to the preindustrial simulation. The ice-free and ice-covered regions here refer to the diagonal hatched and cross-hatched regions in Figure 2c, respectively. The blue line is the linear regression on the ice-covered scatter points, and the response coefficient ( $\lambda$ ) and correlation coefficient ( $r$ ) are just for the ice-covered areas.



725 | **Figure 10.** The monthly response coefficients ( $\text{Wm}^{-2}$ ) of sensible and latent heat fluxes to the insulation effect of sea ice.

## Supplementary Information

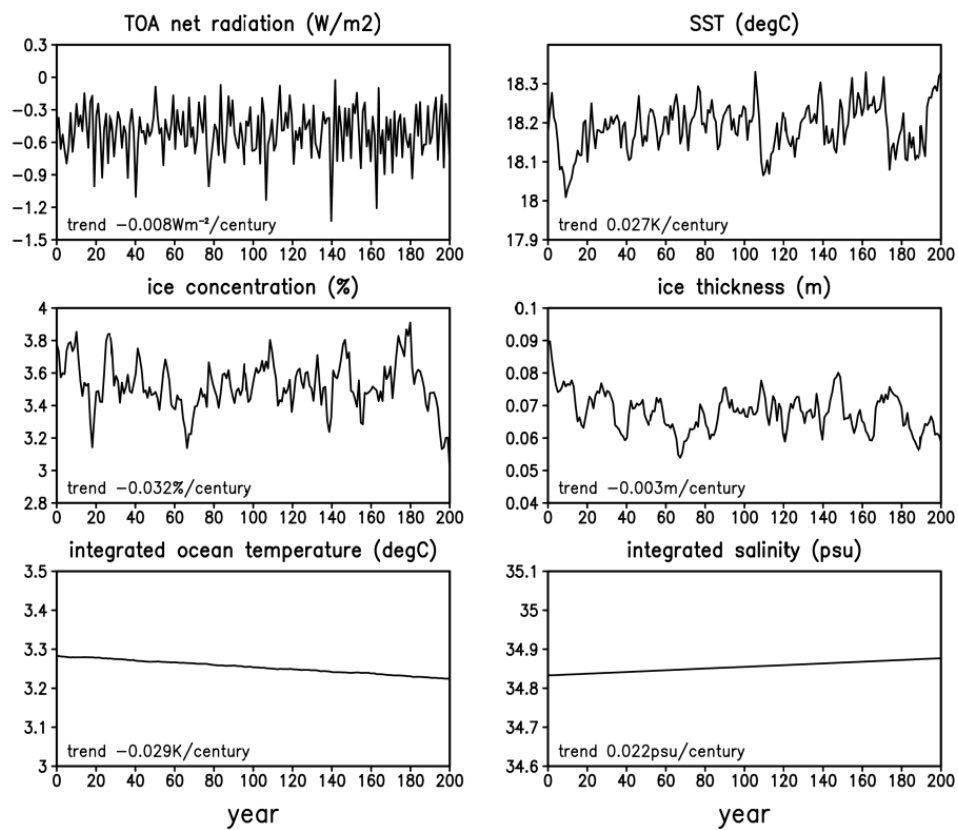


**Figure S1.** The global annual mean of last 200 model years output in the Pliocene simulation (The negative TOA net radiation represents a heat loss of the earth-atmosphere system.)



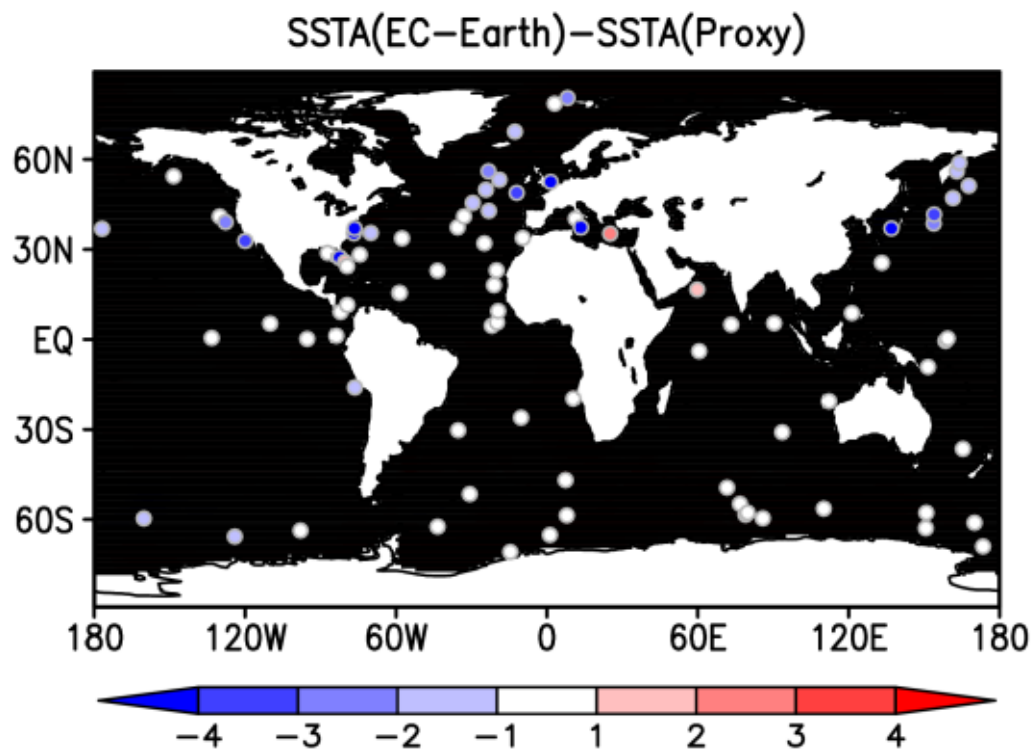


**Figure S2.** The difference of annual mean SST anomaly (Pliocene minus preindustrial, K) between EC-Earth simulation and the proxy data at 95% confidence-assessed marine sites from Deep Sea Drilling Project (DSDP) and Ocean Drilling Program (ODP).

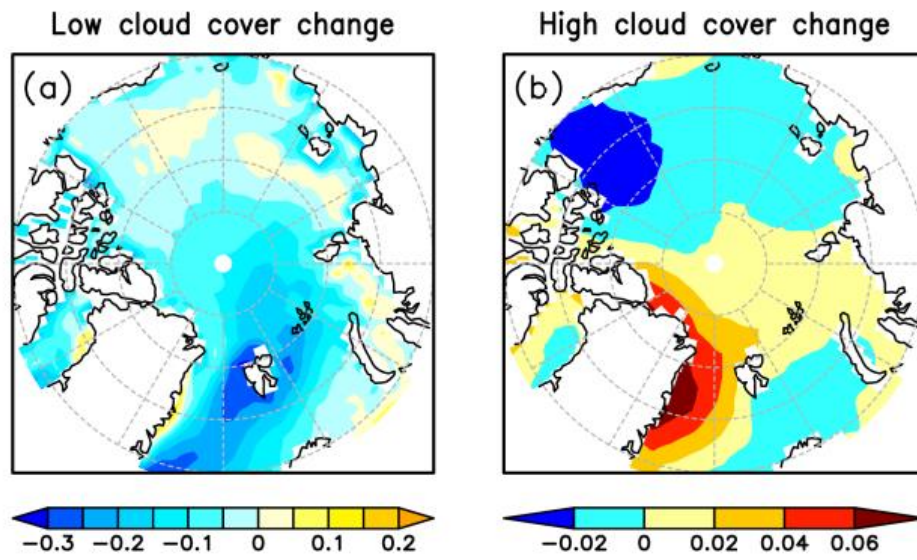


**Figure S3.** The difference of annual mean low cloud cover (a) and high cloud cover (b) anomaly in Pliocene with respect to the preindustrial.